



Effects of ply drops on the fatigue resistance of composite materials and structures
by Mark Ethan Scott

A thesis submitted in partial fulfillment of the requirements for the degree of Master of Science in
Chemical Engineering
Montana State University
© Copyright by Mark Ethan Scott (1997)

Abstract:

Material thickness variations are required to optimize the design of laminated composite structures. These thickness variations are accomplished by dropping layers of material (plies) along the structure to match the load carrying requirements. Unfortunately, these ply drops produce internal stress concentrations as a consequence of material and geometric discontinuities. This thesis provides a parametric experimental investigation of ply drops in E-Glass stranded fabric reinforced polyester composites and structures. These parameters include: ply drop location, laminate thickness, number of plies dropped at one location, fabric type, loading condition, fiber content, and spacing between ply drops. The damage which develops at ply drops is typically delamination cracks which propagate between the layers of reinforcing fabric.

There were two parts to this study: (1) to examine delamination propagation rates at ply drops and determine crack growth threshold levels, and (2) to determine the effect of ply drops on the lifetime of various composite materials. Tests were conducted on both small coupons of material and beam structural elements with ply drops in the flanges.

A strong sensitivity to ply drop position and manufacturing details is shown for fatigue damage initiation and growth. The results indicate that it will be difficult to completely suppress damage and delamination initiation in service. For 0° plies, single internal ply drops provide the greatest delamination resistance. Multiple ply drops should be spaced at correct intervals so that the delaminations from each do not overlap prior to arrest. It was found that, in most cases, there is a threshold loading under which little growth after initiation is noted. Delamination retardation techniques such as ply edge feathering, "Z-Spiking" and adhesive layers improve the delamination resistance in many cases. After delamination has occurred, especially with exterior ply drops, it can be repaired with adhesives. Ply drops adversely affect fatigue lifetime of low fiber content laminates more severely than for high fiber content laminates. The choice of fabrics used in a laminate can have a significant impact on delamination rates, but the lifetime of the laminate is insensitive to fabric type.

EFFECTS OF PLY DROPS ON THE FATIGUE RESISTANCE
OF COMPOSITE MATERIALS AND STRUCTURES

by

Mark Ethan Scott

A thesis submitted in partial fulfillment
of the requirements for the degree

of

Master of Science

in

Chemical Engineering

MONTANA STATE UNIVERSITY
Bozeman, Montana

August 1997

N378
SC085

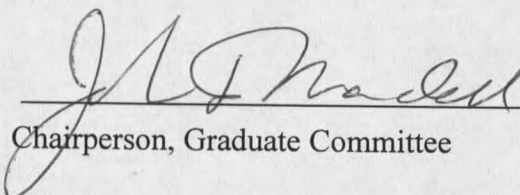
APPROVAL

of a thesis submitted by

Mark Ethan Scott

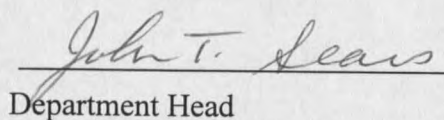
This thesis has been read by each member of the thesis committee and has been found to be satisfactory regarding content, English usage, format, citations, bibliographic style, and consistency, and is ready for submission to the College of Graduate Studies.

Dr. John Mandell

 8/14/97
Chairperson, Graduate Committee Date

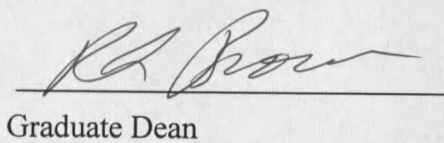
Approved for the Department of Chemical Engineering

Dr. John Sears

 8-15-97
Department Head Date

Approved for the College of Graduate Studies

Dr. Robert Brown

 8/18/97
Graduate Dean Date

STATEMENT OF PERMISSION TO USE

In presenting this thesis in partial fulfillment of the requirements for a master's degree at Montana State University, I agree that the Library shall make it available to borrowers under rules of the Library.

If I have indicated my intention to copyright this thesis by including a copyright notice page, copying is allowable only for scholarly purposes, consistent with "fair use" as prescribed in the U.S. Copyright Law. Requests for permission for extended quotation from or reproduction of this thesis in whole or in parts may be granted only by the copyright holder.

Signature M. Echan Scott
Date 8/18/97

ACKNOWLEDGMENTS

I would especially like to thank Dr. Mandell and Dr. Cairns for their insight and direction. Dan Samborsky receives special thanks for all his time and suggestions with editing figures, efforts in helping with experiments and keeping the facilities running. Zane Maccagnano for his work using finite element analysis to back up the results obtained experimentally. To all of the students in the composites group for their input and good sense of humor during the frustrating moments of school and research. And finally, to my family who have always encouraged and supported me.

This work was supported by the U.S. Department of Energy and the State of Montana through the Montana DOE EPSCoR Program (Contract # DEFC02-91ER75681) and the National Renewable Energy Laboratory (Subcontract # XF-1-11009-5), and Sandia National Laboratories (Subcontract ANO412).

TABLE OF CONTENTS

LIST OF TABLES	vii
LIST OF FIGURES	ix
ABSTRACT	xii
1. INTRODUCTION	1
2. BACKGROUND	4
Strain Energy Release Rate	4
Tensile Testing of Dropped-Ply Laminates	8
Compression Testing of Dropped-Ply Laminates	9
Damage Accumulation	10
Stress Analysis on Dropped-Ply Laminates	11
Delamination Prevention	13
Existence of a Resin Rich Region	14
Design Considerations	15
Motivation for Thesis	18
3. EXPERIMENTAL METHODS AND MATERIALS	20
Test matrix and description of specimens	20
Material Preparation	29
Fabrics	31
Specimen Preparation	32
Test Facility and Development	33
DCB and ENF test specimens	35
4. RESULTS AND DISCUSSION	37
Delamination Study	37
Effect of Ply Drop Location	37
Effects of laminate thickness and multiple ply drops at the same position	43
The ESE and ESF laminates	44
Effect of Ply Drop Spacing	45
Effects of "Z-Spiking"	48
Effect of Tough Adhesive at Ply Drop	49
Effect of Butt-Joints	50
Effects of $\pm 45^\circ$ Ply Drops	51
Effect of A130 warp unidirectional fabric	52
Other attempts to prevent delamination	53

Repairing Delaminated Samples	55
Comparing different laminates	56
Effect of Ply Drops on Lifetime	57
Fiber Volume Content Effect	57
A130 fabric vs. D155 fabric	59
Resin Rich Region	62
Compression Testing	64
Residual Strength of Coupons	67
Ply Drops in Beams	70
Beam Geometry, Fabrication and Materials	70
Flange laminate ESA	73
Beam 39	73
Beam 44	76
Beam 48	78
Flange laminate ESB	80
Beam 40	80
Flange laminate ESG	81
Beam 41	81
Beam 42	85
Flange laminate ESH	86
Beam 49	86
Beam 50	89
Comparison of Delamination Rate in Beams and Coupons	90
Strain Energy Release Rate and Modeling Results	94
Determination of Critical Strain Energy Release Rate	94
Static and Threshold Strain Energy Release Rates at Ply Drops	97
 5. CONCLUSIONS AND RECOMMENDATIONS	 100
Conclusions	100
Delamination at Ply Drops	100
I-Beam Study	101
Effect of Ply Drops on Lifetime	101
G _c Tests	102
Recommendations	102
 REFERENCES	 103
 APPENDIX A	
Coupons Tested	108
 APPENDIX B	
Delamination Length vs. Cycles for Coupons	118

LIST OF TABLES

Table	Page
1. Lay-up of fiberglass materials with Ply Drops	22
2. Test matrix	24
3. Comparison of delamination resistance of different ply drop configurations.	42
4. Slenderness ratios calculated using Equation 4	65
5. Comparison of ESH laminate compressive strength with and without ply drops.	66
6. Residual strength of ESH laminate after being fatigued (R=0.1)	69
7. List of I-beams tested with ply drops	72
8. Reference notation for Beams 39, 44 and 48 with ESA Laminate	74
9. Delamination length vs. fatigue cycles for Beam 39	75
10. Average delamination length vs. cycles for compression and tension flanges for Beam 44.	77
11. Delamination length vs. cycles for tension and compressive flanges on Beam 48. ...	79
12. Reference notation for Beam 40 with ESB laminate	81
13. Reference notation for Beams 41,42 with ESG laminate	83
14. Cycles vs. average tension and compression flange delamination length for beam 41	84
15. Cycles vs. average tension flange delamination for Beam 42.	85
16. Cycles for tension and compression flange delamination on beam 49.	87
17. Reference notation for Beams 49 and 50 with ESH laminate.	88
18. Cycles vs. tension flange delamination length for beam 50.	91

19. Critical strain energy release rate for Mode I and Mode II cracks	97
20. ESA and ESB critical static strength.....	97
21. Static strain energy release rates	98
22. Threshold strain energy release rates	99

LIST OF FIGURES

Figure	Page
1. Common structural elements with discontinuities from Ref. 1	2
2. The three modes of fracture from Broek [2]	5
3. Typical load vs actuator displacement for DCB specimen.	7
4. Typical load vs actuator displacement for a ENF specimen.	8
5. Cross-sectional and edge view of ESB laminate showing ply drop.	28
6. Different delamination prevention techniques.	30
7. Lay-up of laminate with ply drops in mold	31
8. DCB and ENF specimens	35
9. Delamination of exterior zero degree ply drop.	38
10. Typical static failure of laminate with ply drop.	38
11. Delamination length vs. cycles for ESA laminate, $R = 0.1$, Exterior 0° Ply Dropped	39
12. Delamination at an interior ply drop showing two delamination fronts.	39
13. Delamination length vs cycles for ESB (Single interior 0° ply drop) laminate, $R=0.1$	40
14. Delamination length vs. cycles for ESC (Single center interior 0° ply drop) laminate, $R=0.1$	41
15. Illustration of resin rich region in ESH laminate.	45
16. Delamination length vs. cycles for laminates ESB, ESH, ESF (all interior ply drops) at a maximum running stress of 275 MPa, $R=0.1$	46

17. Effect of different spacing between ply drops, R=0.1, ESI laminate (Two, 0° ply drops) at 276 MPa, $V_f=0.35$	47
18. ESI coupons run at 276 MPa, R=0.1.	47
19. Delamination length vs. cycles for ESJ "Z-Spiked" laminate compared to ESA (Single, exterior 0° ply drop) laminate, R= 0.1.	48
20. Delamination length vs. cycles for laminates ESA, ESK, ESG, ESE (all exterior ply drops) at a max. running stress of 138 MPa, R=0.1.	49
21. ESL laminate in tension at the ply drop (Interior 0° ply drop with Hysol adhesive) failed at 276 MPa.	50
22. Delamination length vs. cycles for ESA, JKA "Feathered" and JKA random laminates at a maximum running stress of 207 MPa, R=0.1.	53
23. Delamination initiating along tows which were pulled out.	54
24. Delamination length vs. cycles for ESB and JKB "Feathered" at a maximum running stress of 275 MPa, R=0.1.	54
25. Delamination length vs. cycles at 207 MPa, R=0.1, initial ESA laminate compared to repaired ESA laminate.	55
26. Effect of fiber content on the normalized S-N Data, R=0.1, for DD materials [0/±45/0]s compared to ESH laminate (Two interior 0° Ply drops).	58
27. S-N curve (R=0.1) comparing D155 Fabric (DD6) to A130 Fabric (DD11) control materials with no ply drops, from Reference 50.	60
28. Fatigue life of ESH (Two D155 ply drops) vs. ESQ (Two A130 ply drops) laminates (Maximum stress is on the thin side of the ply drop).	60
29. Tensile fatigue S-N data for ESQ (Two 0° internal ply drops) vs. control DD11 (no ply drops) laminates, A130 unidirectional fabric.	61
30. Damage developing around thermoplastic beads as a result of fatigue loading, R=0.1.	62
31. Photomicrograph of ESH laminate showing resin rich regions ahead of ply drops.	62

32. Side view of crack propagating through ESH laminate	63
33. Tensile fatigue (R=0.1) S-N curves for ESB (Single 0° internal ply drop) and ESH (Two interior 0° ply drops).	63
34. Compressive stress vs. percent strain for ESH 804 coupon.	65
35. I-Beam testing apparatus	71
36. Beam coordinate system	71
37. Beam 39 with ESA laminate for flange material.	76
38. Tension and compression flange on Beam 44.	78
39. Beam 48, ESA laminate, tension and compression flanges.	80
40. Beam 40	82
41. Beam 41	84
42. Beam 42, ESG laminate (Two exterior 0° ply drops) on flanges	86
43. Beam 49 with ESH (Two internal 0° ply drops) flange material.	89
44. Beam 50 with ESH (Two interior 0° ply drops) laminate as flange material.	90
45. Beam (Tension Flange) vs. Coupon Data (R=0.1) for ESA (Single exterior 0° ply drop), R=0.1.	92
46. Beam (tension flange) vs. coupon data for ESH laminate (Two Interior ply drops), R=0.1.	92
47. Mode I coupon geometry.	95
48. Mode II specimen geometry.	96

ABSTRACT

Material thickness variations are required to optimize the design of laminated composite structures. These thickness variations are accomplished by dropping layers of material (plies) along the structure to match the load carrying requirements. Unfortunately, these ply drops produce internal stress concentrations as a consequence of material and geometric discontinuities. This thesis provides a parametric experimental investigation of ply drops in E-Glass stranded fabric reinforced polyester composites and structures. These parameters include: ply drop location, laminate thickness, number of plies dropped at one location, fabric type, loading condition, fiber content, and spacing between ply drops. The damage which develops at ply drops is typically delamination cracks which propagate between the layers of reinforcing fabric.

There were two parts to this study: (1) to examine delamination propagation rates at ply drops and determine crack growth threshold levels, and (2) to determine the effect of ply drops on the lifetime of various composite materials. Tests were conducted on both small coupons of material and beam structural elements with ply drops in the flanges.

A strong sensitivity to ply drop position and manufacturing details is shown for fatigue damage initiation and growth. The results indicate that it will be difficult to completely suppress damage and delamination initiation in service. For 0° plies, single internal ply drops provide the greatest delamination resistance. Multiple ply drops should be spaced at correct intervals so that the delaminations from each do not overlap prior to arrest. It was found that, in most cases, there is a threshold loading under which little growth after initiation is noted. Delamination retardation techniques such as ply edge feathering, "Z-Spiking" and adhesive layers improve the delamination resistance in many cases. After delamination has occurred, especially with exterior ply drops, it can be repaired with adhesives. Ply drops adversely affect fatigue lifetime of low fiber content laminates more severely than for high fiber content laminates. The choice of fabrics used in a laminate can have a significant impact on delamination rates, but the lifetime of the laminate is insensitive to fabric type.

CHAPTER 1

INTRODUCTION

Today's need for stronger, lighter and cheaper structures has generated much interest in materials development, especially in composite materials. Fiber-reinforced composites have played a leading role in the technological advancement of structural material systems. Typically, fiber-reinforced composites are known for being light weight, high strength materials which are more durable than conventional materials. The use of composite materials in structural applications is rapidly increasing for commercial applications. With this increased use comes the need for a better understanding of the performance of the structures fabricated from composite materials, called composite structures. A large portion of composite structures are comprised of layered, laminated composite materials; thickness variations in such laminates are achieved by changing the number of plies in proportion to the thickness change. This requires the termination of layers, or plies, within the laminate, which then introduces a characteristic flaw into the material.

Laminated composites typically are fabricated from planar sheets of material, so that all fibers are oriented in a plane. Careful design and selection of the in-plane fiber

orientation can create a laminate that is designed to carry the loads very efficiently in the plane of the fiber reinforcement. However, an inherent weakness of the laminate is the lack of fiber reinforcement in the direction normal to the fiber orientation. Consequently, the interlaminar direction, normal to the plane of reinforcement, is the weakest direction of the laminated material system. Therefore, any interlaminar loads that are applied to or induced within the structure are of particular concern in terms of structural integrity.

Figure 1, from Ref. 1, illustrates five structural elements used in laminated composite structures that produce interlaminar stresses. These common elements are the free edge, the open hole, the ply drop, and bonded or bolted joints. Free edges are unavoidable in many structures. Open holes are commonly employed to allow access to the internal parts of the structure. When the design calls for a laminate that is tapered in thickness, discontinuous layers or plies are utilized. It is also common to insert

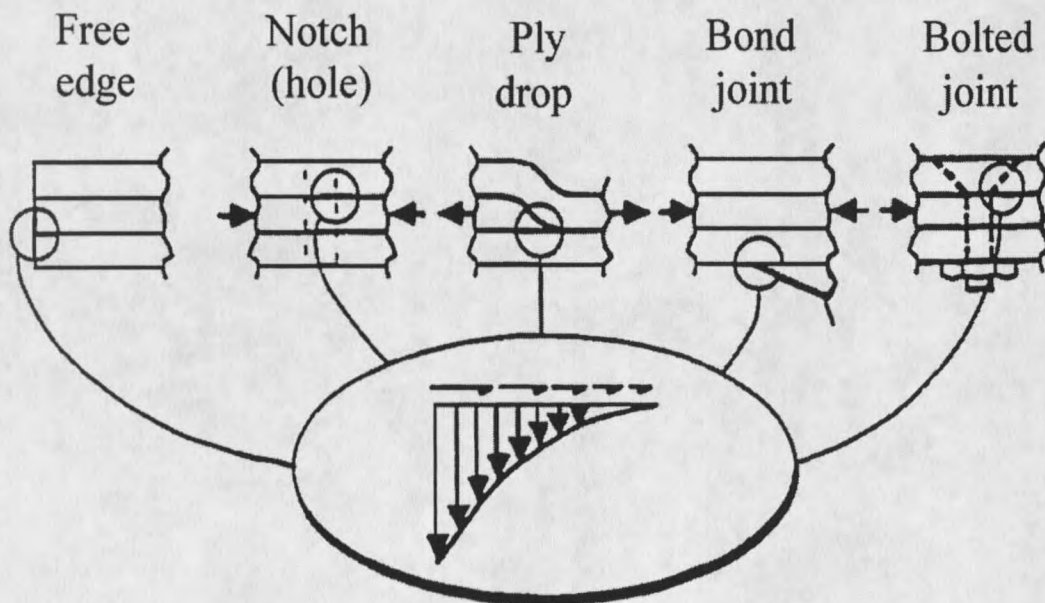


Figure 1. Common structural elements with discontinuities from Ref. 1

discontinuous plies to create a local build-up or thickening at high stress points. Finally, bonded or bolted joints are required to attach multiple sub-components of the structure.

Each of the structural elements shown in Figure 1 develop significant out-of- plane normal and shear forces when the component is under load. These interlaminar loads are acting on the plane of minimum strength and toughness of the laminated structure.

Therefore, each of these structural elements have the potential to cause a delamination of the individual layers. In addition, most analyses and failure models do not account for these interlaminar loads. The interlaminar performance of these critical structural elements provides a limit to the structural performance of the composite structure. It is important to note that the approach taken in this thesis is also directly applicable to some degree to all of the interlaminar stress risers illustrated in Figure 1.

The approach in this work was to focus on the ply-drop configuration. This is an unavoidable flaw if the thickness is to be tapered, and has received limited attention in the literature with respect to low cost composites of this type under fatigue loading. A parametric experimental study of the influence of various geometric details of ply drops was carried out using laminate coupons, in terms of both the delamination resistance and the reduction in fatigue lifetime. The work is then extended to ply drops in the flanges of larger I-beam structures.

CHAPTER 2

BACKGROUND

This Chapter reviews the basic mechanics of delamination in terms of the strain energy release rate. Several key problem areas associated with thickness transitions in composite laminates are then identified and discussed. Issues in need of an increased research effort are identified.

Strain Energy Release Rate

Once a crack is initiated in a structure it can be further propagated in any of three different modes, or a combination of these. Figure 2 shows the three modes of crack growth. Mode I is an "opening mode" crack, which is caused by normal stresses. In-plane shear causes Mode II or "sliding mode" cracks and Mode III cracks are caused by out-of-plane shear and are known as "tearing mode" cracks [2].

The strain energy release rate, G , is based on the Griffith criterion [2]. Griffith stated that crack propagation will occur if the energy released upon crack growth is sufficient to provide all the energy that is required for crack growth. The Griffith equation can be represented as

$$\frac{dU}{da} = \frac{dW}{da} \quad (1)$$

where U is the elastic strain energy and W the energy required for crack growth. G is equal to dU/da and is sometimes called the crack driving force. The energy consumed during crack propagation is denoted by R , which is equal to dW/da , and is called the crack resistance. Thus, R is equal to the critical strain energy release rate to cause crack extension.

There is a different critical strain energy release rate for each mode of crack growth. A subscript denotes the particular mode. The critical strain energy release rate is

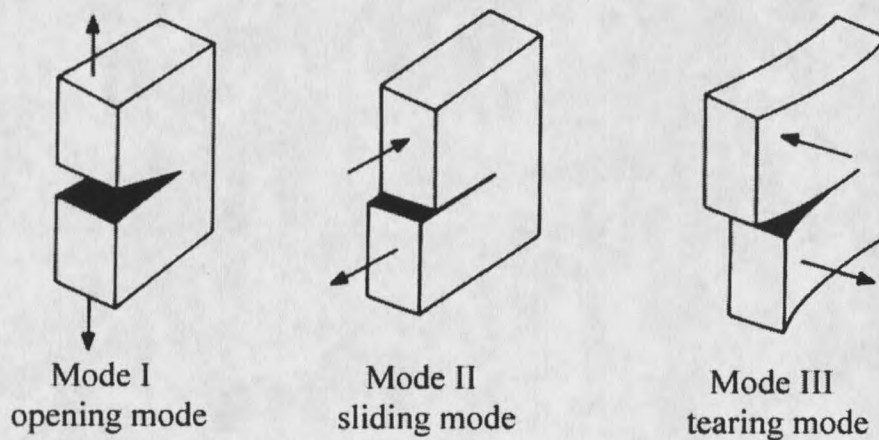


Figure 2. The three modes of fracture from Broek [2].

denoted with a “c” in the subscript following the mode designation. Above this value of G , in simple linear elastic fracture mechanics [2], a crack will propagate unstably in the structure. If there is a mechanism which produces increased crack resistance as the crack

extends, the crack will propagate according to some R-curve behavior, requiring higher G values as crack extension occurs [2].

To determine an opening mode, or Mode I, strain energy release rate for delamination, a double cantilever beam (DCB) specimen is used. The critical strain energy release rate can be obtained by determining the area enclosed by the loading and unloading curves on a load-displacement diagram, which is the incremental change in stored strain energy, U , with crack extension Δa . A typical loading-unloading diagram for a DCB specimen can be seen in Figure 3. Another method to determine G_I values

$$G_{Ic} = \frac{12P_c^2 a^2}{EB^2 h^3} \quad (2)$$

uses an analytic formula (Eq. 2) proposed by Benbow and Roesler [3] and Gilman [4] which takes into account the strain energy generated due to the bending moment of the DCB test, where a is the crack length, E the modulus parallel to the crack direction, B the laminate width, h is the half height and P_c is the critical load. Many G values can be obtained from a single DCB specimen which allows a crack resistance (R) curve to be generated, indicating how (and if) the resistance to crack growth changes with increasing crack length.

To determine Mode II crack growth resistance, it is necessary to use a different test method to determine the corresponding strain energy release rate. End notched flexure (ENF) tests apply a load to the center of the coupon; when the applied load

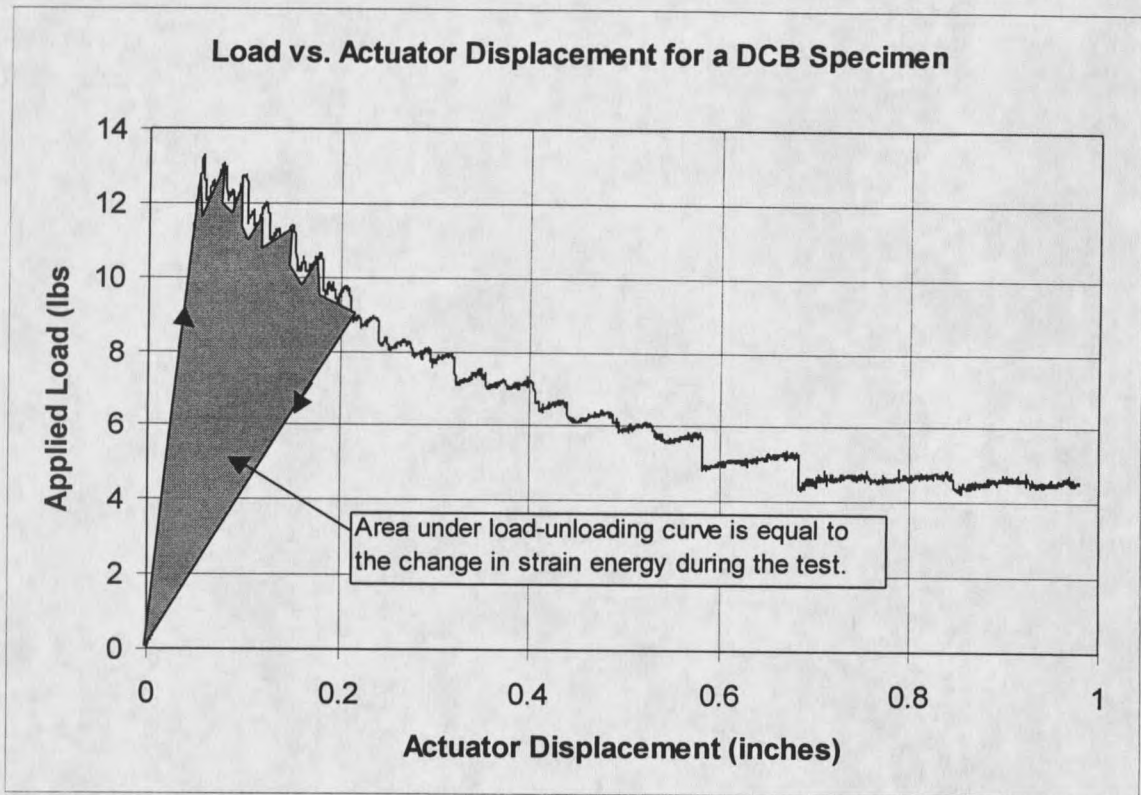


Figure 3. Typical load vs. actuator displacement for DCB specimen.

reaches a critical value, the crack propagates suddenly toward the center where the load is applied. In this type of test, there is only one data point collected as compared with the many points for the DCB specimen due to the instability of crack growth in the ENF specimen. A typical load-actuator displacement graph is shown in Figure 4. Since the load-displacement diagram is unstable for Mode II tests, an analytic formula is necessary to determine a G value. The formula proposed by Russell and Street [5] to calculate G_{IIc} is

$$G_{IIc} = \frac{9P_c^2 a^2}{16E_x w^2 h^3} \quad (2)$$

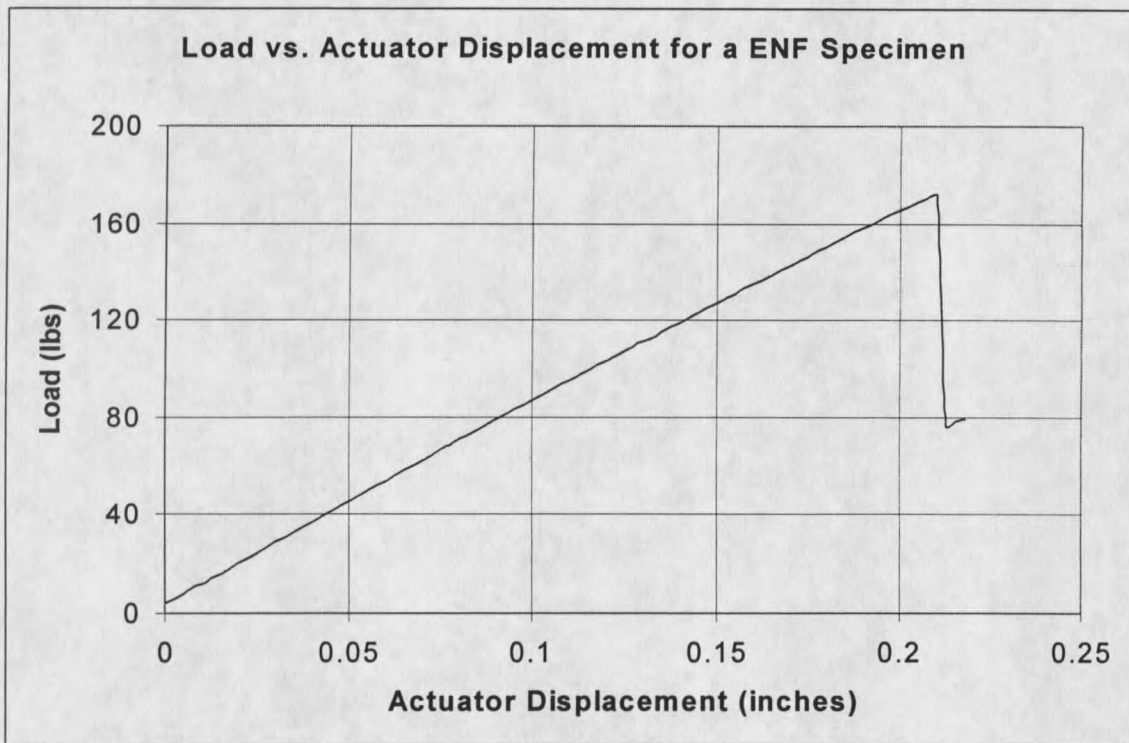


Figure 4. Typical load vs. actuator displacement for a ENF specimen.

Where P_c is the critical applied load, a is the initial crack length, E_x is the modulus in the long direction of the specimen, w is the width of the specimen and h is the half thickness of the specimen.

Tensile Testing of Dropped-Ply Laminates

The DCB and ENF specimens are used to induce crack growth in pure Mode I and II, respectively. Ply drops do not cause a pure mode of crack growth, but generally display a combination of at least Modes I and II, as discussed later. Lagace and Cannon [6] conducted an experimental program investigating the influence of discontinuous internal plies on the tensile response of graphite/epoxy laminates. The fiber orientation was chosen to minimize the occurrence of the edge delamination failure mode. For the

configurations investigated, little change in the global stress-strain behavior and ultimate load carrying capability were observed relative to similar constant thickness laminates. The work illustrated an effect due to the placement of multiple ply drop-offs. When discontinuous plies were distributed along the specimen length, the laminate failed similar to a laminate without ply drops. However, when multiple plies were dropped at one position in the laminate, a delamination failure resulted. It was suggested that the apparent penalty in the in-plane response may be more severe for compression loading.

Wisnom [7] looked at the size effect of coupons on delamination rate. Larger size coupons showed a decreasing delamination rate. Also, when the number of plies dropped in one location was increased, there was a significant increase in the rate of delamination.

The effect of the fiber content on ply drop effect has not received much attention. The apparent reason for this lack of research is that the majority of work has been centered around the use of pre-preg laminates which generally have ply thicknesses of less than 0.2 mm, with fiber volume contents ranging narrowly in the fifty to sixty percent range. The fiberglass laminates being studied for use in this project ranged in fiber content from the low thirties to the mid-fifty percent range. Mandell, et al. [8] showed that the tensile fatigue resistance decreases with increasing fiber content. The cause of this is postulated as due to the decreased amount of resin between plies which acts as a buffer to reduce stress concentrations resulting from matrix cracks in adjacent layers.

Compression Testing of Ply Drop Laminates

Grimes and Dusablon [9] investigated the static and fatigue compression behavior of graphite/epoxy composites with internal ply drop-offs subjected to severe operating

environments. A $[\pm 45/0/90]_s$ family laminate with up to four dropped plies was tested. The static strength and stiffness were insignificantly affected by the discontinuities. However, the endurance limit was decreased by up to 30 percent depending on the orientation of the discontinuous layers.

Curry, et. al. [28] noted that dropped plies can cause a significant reduction in compressive strength. Also, the greater the change in axial stiffness between the thick and thin sections, the greater the reduction in strength. The reduction in compressive strength is much greater than the reduction in tensile strength.

Damage Accumulation

Ulman et al. [10] conducted an extensive experimental program with graphite/epoxy laminates with single ply drops. Damage initiation and growth from both open holes and ply terminations were evaluated during both static testing and constant amplitude fatigue testing of a $[0/\pm 45/90]$ family laminate. The results indicated that although the loading mode greatly influenced the damage development process, interfacial delamination was present in both static and fatigue loading before ultimate failure. Tapered specimens were shown to be dominated by the ply drop. Under tensile loads, the damage progressed from matrix cracking in the resin-rich zone, to transverse cracks at the ply termination. Continued loading induced delamination which increased in size until final failure. In fatigue loading, the damage development was similar, but, delamination growth dominated the last 75 percent of the structural life. A similar fracture response was illustrated for compression loading; however, the process occurred much more rapidly.

Reifsnider [11] showed that the residual (remaining) strength of typical composites does not deteriorate from the static value until a few hundred cycles before failure. This was because the accumulated damage in fatigue samples was similar in type and amount to that in quasi-static tests near failure.

Stress Analysis of Ply Drop Laminates

A numerical study of a 30-ply carbon fiber laminate containing two zero degree dropped plies at different locations through the thickness was performed by Adams, et al. [12]. A three-dimensional finite element analysis incorporating nonlinear orthotropic lamina properties was conducted to assess the effect of compressive load, moisture and temperature. Although the residual thermal stresses resulting from post cure cooling were found to be significant, the interlaminar stresses were negligible compared to the in-plane stresses. It was concluded that the dropped plies have little effect on the in-plane stresses.

Kemp and Johnson [24] presented a failure analysis of an eight-ply quasi-isotropic graphite/epoxy laminate containing up to three dropped zero degree plies, in a single drop step. The finite element method was applied to determine the resulting three-dimensional state of stress. Interlaminar stresses were found to be significant at the location of the dropped plies. In-plane failure loads were calculated based on both resin failure near the dropped plies and intralaminar failure in tension and compression. A maximum principal stress criterion was applied to predict resin failure and the Tsai-Wu criterion was applied to predict intralaminar failure. The analysis predicted initial failure to occur in the resin. No experimental data was generated to correlate with the numerical results.

Curry et al. [28] studied sixteen-ply graphite/epoxy laminates, containing four plies terminated at the mid-plane. A stress based failure theory was applied to predict the axial compressive strength. The results were shown to under estimate experimentally determined failure loads by 33 percent. Experimental results indicated that both the tensile and compressive strength are reduced by the presence of a thickness discontinuity. However, the reduction was larger for compressive loading. In addition, the reduction in strength was shown to be inversely related to the increase in axial stiffness of the thick section relative to the thin section.

Fish and Lee investigated the tensile strength of tapered glass/epoxy laminates with multiple internal ply drops [13]. A three-dimensional finite element analysis was conducted and the average stress concept was applied to predict the initiation of failure. Strength predictions, based on the stress in the inter-ply resin layers and an averaging distance of one ply thickness, were found to correlate with the experimentally observed delamination failure. However, the predictions were valid only for delamination initiation and not delamination growth. Laminates both with and without significant edge effects were tested. The failure mode for those with negligible free edge effects was an unstable delamination growth across the width of the laminate, followed by stable delamination growth in the axial direction. One of the tapered laminates showed an increase in strength while the other showed a decrease. Alternatively, laminates containing 90° plies showed a significant free edge effect. The corresponding failure mode was a combination of free edge delamination and delamination growth in the axial direction [14].

A similar analysis for laminates with external ply drop-offs was conducted by Wu and Webber [15]. A two-dimensional finite element analysis was performed.

Interlaminar peel and shear stresses were found to peak in the corner regions of the external steps. The failure of the laminates in delamination was attributed to these peak stresses.

Unidirectional glass/epoxy and graphite/epoxy laminates with internal drop-offs were studied by Hoa et al. [16]. Under tensile loading, the laminates failed in delamination at load levels well below the in-plane strength. Stress and strain variations within the taper were obtained using a three-dimensional finite element model employing a quadratic displacement based element. An acoustic emission was found to correspond to the initiation of delamination while no change in the stress-strain response was observed. Reasonable correlation between experimental and numerical results was reported when the interlaminar stresses were compared to the interlaminar strength of the material.

Delamination Prevention

Another type of ply drop occurs in laminates with discontinuous interlaminar layers in the use of buffer strips [17,18]. A buffer strip is added or constructed by either discontinuing specific fiber layers of a laminate, usually the stiff zero degree plies, or inserting additional plies of lower longitudinal modulus. The objective is to create discrete region of increased local compliance within the component. The result is a superior construction in terms of damage tolerance. As damage in the main laminate grows, it can be arrested and controlled by the more compliant buffer strips. Such a

construction has been shown to reduce the sensitivity of composite structures to inherent damage and to increase the lifetime of the component [19].

Another method currently being used is called "Z- Spiking". Aztex Co. (Waltham, Mass.) uses fibers positioned in foam which is then vacuum pressed into the laminate to reinforce laminates in the thickness direction. This reinforcement is especially useful for bonded joints, where the strength of the joint is matrix dominated. Aztex [20] reports a minimal decrease in the in-plane properties and a 30-fold increase in interlaminar fracture toughness. Tanzawa [21] showed that although the z reinforcing fiber content was approximately 0.6%, the normally brittle carbon fiber/epoxy plates had the same critical strain energy release rate as carbon fiber/PEEK plates. By increasing the critical strain energy release rate, the structure becomes more delamination resistant without having to increase the cost by using the more expensive PEEK thermoplastic matrix.

Chan [22] used narrow, tough thermoplastic interlayers to prevent coupon edge delamination. In another study, Masters [23] used an entire layer of adhesive to improve the impact toughness of composites. These interlayers provided a tough region where propagating cracks could be arrested before growing long enough to cause a catastrophic failure in the component.

Existence of a Resin Rich Region

It has been shown that during processing of a variable thickness laminate, a pure resin region develops at the end of the discontinued plies. Therefore it is the resin flow from surrounding layers during processing that creates this neat resin zone. After the

resin fills the mold, porosity can become entrapped in the resin in this area creating stress concentrations which can initiate delamination. The volume and dimensions of this region are clearly a function of the number of discontinuous layers at a given location and the orientation of the surrounding layers. The existence of this neat resin region has been observed in several works [24-28]. A common method employed to account for this micro structural detail is to inspect actual laminates with photo microscopy. Although this identifies the size and shape of the neat resin zone, there has been little effort to address the change in fiber volume content near a discontinuous layer. Chan and Ochoa [26] did attempt to account for the change in ply properties that occur local to the discontinuous plies.

Design Considerations

In metallic structures, damage tolerance technology has been used effectively to characterize crack growth under cyclic loading for a material, predict the rate of crack growth in the structure under service loads, and establish inspection intervals and nondestructive test procedures to ensure operational safety [29]. Because composite delamination represents the most commonly observed macroscopic damage mechanism in laminated composite structures, many efforts have been undertaken to develop similar procedures for composite materials by characterizing delamination growth using fracture mechanics [30-33]. Although this approach is promising, there are some fundamental differences in the way fracture mechanics characterization of delamination in composites may be used to demonstrate fail safe designs compared with the classical damage tolerance treatment used for metals.

Many papers have been published recently where the rate of delamination growth rate with fatigue cycles has been expressed as a power law relationship in terms of the strain energy release rate, G , associated with delamination growth [1-4]. This fracture mechanics characterization of delamination growth in composites is analogous to that of fatigue crack growth in metallic structures, where the rate of crack growth with cycles is correlated with the stress intensity factor at the crack tip. However, delamination growth in composites, with a relatively high crack growth exponent, may change too rapidly over too small a range of load, and G , to be incorporated into a classical damage tolerance analysis for fail safe designs [2,34,35]. Where in metals the range of fatigue crack growth may be described over as much as two orders of magnitude in G , the growth rate for a delamination in a composite is often characterized over less than one order of magnitude in G . Hence, small uncertainties in applied loads may yield large (order of magnitude) changes in delamination growth. Different damage mechanisms may also interact with the delamination and increase the resistance to delamination growth. Delamination growth resistance curves may be generated to characterize the retardation in delamination growth from other mechanisms [36,37,38]. This delamination resistance curve is analogous to the R-curves generated for ductile metals that account for stable crack growth resulting from extensive plasticity at the crack tip. However, unlike crack tip plasticity, composite damage mechanisms such as fiber bridging and matrix cracking, may not always be present to the same degree.

One alternative to using the classical damage tolerance approach for composites would be to use a strain energy release rate threshold, below which no delamination

growth occurs, and design to stress levels below this threshold. Metals are macroscopically homogeneous, and the initial stress conditions that create cracks at particular locations in preferred directions cannot be easily identified beforehand. Composites, however, are macroscopically heterogeneous, with stiffness discontinuities that give rise to stress risers at known locations such as free edges, internal ply drops, and matrix cracks. Although these stress fields are not the classical variety observed at crack tips, and hence cannot be characterized with a single common stress intensity factor, they can be characterized in terms of the strain energy release rate, G , associated with eventual delamination growth [4].

The most common technique for characterizing delamination onset in fatigue for composite materials is to run cyclic fatigue tests on standard composite specimens, where G for delamination growth is known, at maximum load or strain levels below that required to propagate a delamination monotonically. A strain energy release rate threshold for delamination onset may be developed by running tests at several maximum cyclic load levels and plotting the cycles to delamination onset versus the maximum cyclic G , corresponding to the maximum cyclic load or strain applied[39-43]. This G curve may then be used to determine a threshold value of G for delamination and to predict delamination onset in other laminates of the same material, or at other points [44].

Uncertainty inherent in predicting service loads has generated concern for using a no-growth threshold design criterion for high cycle fatigue applications. If G values exceed no-growth threshold levels, a catastrophic delamination propagation may occur. O'Brien [45] outlines a damage threshold/fail-safety approach for composite fatigue

analysis that involves the following steps:

- 1.) Predict the delamination onset thresholds using fracture mechanics.
- 2.) Assume that surpassing the delamination threshold corresponds to complete propagation.
- 3.) Determine the remaining load carrying capability of the composite with delamination present using composite mechanics (i.e., check for fail-safety).
- 4.) Iterate on Steps 1 to 3 to account for multiple sources of delamination.

Step 1 may be used to demonstrate the delamination durability of any composite structure. Step 2 reflects a way to deal with relatively high exponent delamination growth observed for composites as compared to metals. An alternative would be to predict the delamination growth rate using growth laws that incorporate R-Curve characterization, thereby taking into account the resistance provided by other damage mechanisms. Finally, Step 3 acknowledges that the residual strength of the composite is a function of structural variables, and it is not uniquely a question of material characterization. This proposed damage-threshold fail-safety concept incorporates generic material properties of fracture mechanics and also takes into consideration the unique characteristics of laminated composites.

Motivation for Thesis

Previous research has focused on graphite/epoxy [6] or pre-impregnated E-glass and S-glass [7] laminates containing ply drops. Graphite/epoxy laminates have better fatigue resistance than do glass fiber composites [7]. The pre-impregnated composites usually have thinner plies than do typical laminates of the type used in this study, which

may minimize ply drop effects. To achieve efficient designs, wind turbine blades require severe thickness tapering to reduce the overall weight. Blades are also subjected to very high cycle fatigue loading, which can lead to delaminations over a period of many years. This, along with an absence of adequate data on the effects of ply drops in laminates using the E-glass stranded fabrics typical of blade and other low cost composite applications, gives motivation for this thesis.

CHAPTER 3

EXPERIMENTAL METHODS AND MATERIALS

Test matrix and description of specimens

This section provides a brief overview of the different cases tested. Table 1 gives the lay-up of each case as well as other comments. Table 2 gives the test matrix used to determine the properties of the laminates listed in Table 1, including the number of coupons tested at each stress level, and the loading conditions (tension or compression). In the following paragraphs, plies which are terminated (near mid-length of the coupon) are shown with asterisks. As described later, all laminates were resin transfer molded using stitched or woven fabric reinforcement.

The laminates were based on the DD set of laminates, which exhibited the best fatigue performance of the laminates previously tested [47]. Selected cases of ply drops, both interior and exterior (on the surface), were introduced into laminates. After initial delamination studies with single ply drops were completed, multiple ply drops at the same location, as well as spaced along the length, were also studied. Attempts to suppress delamination with the addition of adhesives, feathering and "Z-Spiking" were then studied. All of these attempts investigated dropping 0° plies. The effect of dropping single and multiple $\pm 45^\circ$ layers was then studied. In addition, A130 woven fabric for the

zero degree layers was also substituted for the standard D155 fabric used in the DD family of laminates.

The ESA laminate included a single exterior zero degree ply drop. The actual configuration of the laminate is $[0^*/0/\pm 45/0/0/\pm 45/0]$, where the angle given is relative to the applied load direction. Ply configurations follow standard laminate notation [46]. The ESB laminate has the configuration $[0/0^*/\pm 45/0/0/\pm 45/0]$, while the ESC laminate has the configuration $[0/\pm 45/0/0^*/0/\pm 45/0]$, with a central ply being terminated. In terms of percentages, the ESA, ESB and ESC laminates have a 14% drop in thickness, with 20% of the zero degree layers being dropped. The ESD laminate has two internal plies being dropped with the laminate configuration $[0/\pm 45/0^*/0^*/\pm 45/0]$. This is a 33% drop in the total thickness, with 50% of the zero degree layers being dropped. Figure 5 shows an actual polished cross-section through an ESB coupon prior to testing. The edge of the ply drop is somewhat smeared during molding, with a resin rich area ahead of the drop. The thickness taper coincides with the ply drop as closely as possible, to give an approximately constant fiber content along the length.

In the next set of laminates thicker materials were used to investigate less severe thickness tapering. The ESE laminate had the configuration $[0^*/(0/\pm 45/0)_3]$, while the ESF laminate incorporated a single internal ply drop into the thicker laminate $[0/0^*/\pm 45/0/0/\pm 45/0/0/\pm 45/0]$. In each of these laminates the thickness was tapered 10%, while the percentage of zeros being dropped was 15%. The ESG and ESH laminates both

Table 1. Lay-up of fiberglass materials with ply drops

Lay up of Fiberglass Materials with Ply Drops		
Laminate	Ply Configuration	Description
ESA	$[0^*/(0/\pm 45/0)_s]$	Single Exterior Ply Drop
ESB	$[0/0^*/\pm 45/0/0/\pm 45/0]$	Single Interior Ply Drop
ESC	$[0/\pm 45/0/0^*/0/\pm 45/0]$	Single Center Ply Drop
ESD	$[0/\pm 45/0^*/0^*/\pm 45/0]$	Double Central Ply Drop
ESE	$[0^*/(0/\pm 45/0)_3]$	Single Exterior Ply Drop, with thicker laminate
ESF	$[0/0^*/\pm 45/0/(0/\pm 45/0)_2]$	Single Interior Ply Drop with thicker laminate
ESG	$[0^*/0^*/(0/\pm 45/0)_3]$	Two exterior ply drops with thicker laminate
ESH	$[0/0^*/0^*/\pm 45/0/(0/\pm 45/0)_2]$	Two interior ply drops with thicker laminate
ESI	$[0/0^*/0^*/\pm 45/0/0/\pm 45/0]$	Two interior ply drops with different spacing between the ply drops.
ESJ	$[0^*/(0/\pm 45/0)_s]$	"Z-Spiking" of a single exterior ply drop.
ESK	$[0^*/(0/\pm 45/0)_s]$	Single exterior ply drop, Hysol EA9309.2NA adhesive applied to ply drop before polyester resin was put in the mold.
ESL	$[0/0^*/\pm 45/0/0/\pm 45/0]$	Single interior ply drop, Hysol EA9309.2NA adhesive applied to ply drop before polyester resin was put in the mold.
ESM	$[0/0^*/\pm 45/0/0/\pm 45/0]$	Attempted "Z-Spiking" with an interior ply drop. The zero degree ply being dropped was slipped through a cut ± 45 layer.
ESN	$[0^{**}/\pm 45/0/0/\pm 45/0]$	Outside zero degree layer used as a butt-joint.
ESO	$[0/\pm 45^{**}/0/0/\pm 45/0]$	Inside $\pm 45^\circ$ degree layer contains a butt-joint.
ESP	$[0/\pm 45^*/\pm 45^*/\pm 45/0/(0/\pm 45/0)_2]$	Two interior $\pm 45^\circ$ layers being dropped.
ESQ	$[0/0^*/0^*/\pm 45/0/(0/\pm 45/0)_2]$	Two interior ply drops with thicker laminate A130 fabric instead of D155 fabric
ESR	$[0/\pm 45/0/\pm 45^*/\pm 45^*/0/\pm 45/0]$	Two interior ± 45 ply drops at the centerline

Lay up of Fiberglass Materials with Ply Drops

Laminate	Ply Configuration	Description
JKA "Feathered"	[0*/(0/±45/0) _s]	Alternating tows were pulled one half inch past the adjacent tows in the ply drop layer.
JKA Random	[0*/(0/±45/0) _s]	Random mat laid down underneath the ply drop
JKB "Feathered"	[0/0*/±45/0/0/±45/0]	Alternating tows were pulled one half inch past the adjacent tows in the ply drop layer.
<p>* Ply being terminated</p> <p>** Ply contains a butt-joint oriented at 90° to the load direction.</p> <p>The subscript s denotes a symmetrical lay-up about the location of s, while the notation ()_n indicates that the lay-up in () is repeated n times [46].</p>		

Table 2. Test matrix

Laminate Configuration	Tension Coupons (R=0.1)*		Compression Coupons (R=10)*	
	Maximum Stress (MPa)	# of Tests	Minimum Stress (MPa)	# of Tests
ESA	Static	6	-207	2
	207	3	-138	2
	138	3		
ESB	Static	4		
	345	2		
	310	3		
	276	5		
ESC	Static	2		
	345	3		
	276	3		
ESD	Static	1		
	138	1		
ESE	Static	2		
	207	2		
	138	2		
	121	1		
ESF	345	1		
	276	4		
	207	1		
ESG	Static	1		
	345	1		
	207	1		
	138	2		
	103	1		

Laminate Configuration	Tension Coupons (R=0.1)*		Compression Coupons (R=10)*	
	Maximum Stress (MPa)	# of Tests	Minimum Stress (MPa)	# of Tests
ESH	Static	8	-276	3
	454	1	-207	2
	414	5		
	345	3		
	276	7		
	207	6		
ESI1	310	1		
	276	3		
ESI2	310	2		
	276	3		
	246	1		
ESI3	276	3		
	241	2		
	207	1		
ESI4	310	1		
	276	4		
	241	1		
ESJ	276	1		
	207	3		
ESK	276	1		
	207	2		
	138	1		
ESL	276	2		
	241	2		

Laminate Configuration	Tension Coupons (R=0.1)*		Compression Coupons (R=10)*	
	Maximum Stress (MPa)	# of Tests	Minimum Stress (MPa)	# of Tests
ESM	276	1		
ESN	276	1		
	172	1		
	138	1		
	103	2		
ESO	345	1		
	310	2		
	276	3		
ESL	Static	3		
	552	2		
	414	3		
	276	3		
	207	1		
ESR	276	2		
	241	2		
JKA "Feathered"	276	3		
JKA Random	276	3		
JKB "Feathered"	276	3		

* R = minimum load/maximum load

included more than one ply drop at the same position. ESG had two exterior zero degree layers dropped while the ESH laminate had two interior plies dropped. The laminate

configurations were $[0^*/0^*/(0/\pm 45/0)_3]$ for the ESG laminate and $[0/0^*/0^*/\pm 45/0/0/\pm 45/0/0/\pm 45/0]$ for the ESH laminate. In both of these laminates the thickness was tapered 18% , while the percentage of zero degree layers being dropped was 25 percent.

The ESI laminate contained multiple single ply drops with each ply drop separated by multiples of 13 mm spans. For example, the ESI2 had a 25 mm spacing between ply drops, while the ESI3 laminate had a 38 mm spacing in between ply drops. The laminate lay-up, $[0/0^*/0^*/\pm 45/0/0/\pm 45/0]$, had a 25% thickness taper while the percent of zeros being dropped was 33%.

ESJ and ESK used special details shown in Figure 7 in an attempt to increase delamination resistance. The ESJ laminate used "Z-Spiking" [47], to provide a thickness reinforcement. This was accomplished by interlacing the exterior zero degree ply drop with a continuous zero degree layer. This helped to prevent the surface ply drop from peeling away when the coupon was loaded. The ESK laminate also was an exterior ply drop; to prevent delamination, a tough epoxy adhesive, Hysol EA 9309.2NA, was applied to the ply drop zero degree layer and the first continuous layer and then allowed to cure before the resin was introduced into the mold. The fabric lay-up for both the ESJ and ESK laminates was the same as for the ESA laminate, $[0^*/0/\pm 45/0/0/\pm 45/0]$. The ESL and ESM laminates considered delamination prevention for internal ply drops. The ESL laminate used the same Hysol adhesive as the ESK laminate. Again the adhesive was applied both underneath and above the ply drop and allowed to cure before the resin was introduced into the fabric. The ESM laminate represents an attempt to "Z-Spike" an

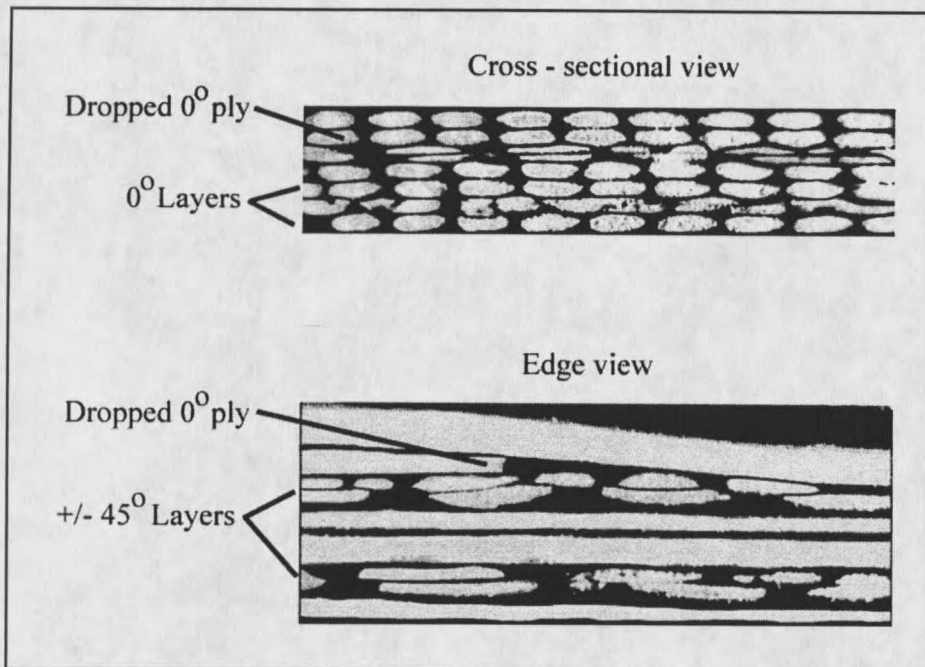


Figure 5. Cross-sectional and edge view of ESB laminate showing ply drop.

internal ply drop. This was accomplished by cutting the $\pm 45^\circ$ degree layer underneath the ply drop and pushing the layer being terminated through the $\pm 45^\circ$ layer. Both of these laminates used the same lay-up as the ESB laminate, $[0/0^*/\pm 45/0/0/\pm 45/0]$.

The ESN and ESO laminates incorporated butt-joints in plies. In order to use some glass fabrics which are only available as weft unidirectionals, butt-joints are necessary. In both the ESN and ESO laminate there are no dropped plies, but the butt joints cause a stress discontinuity similar to the effect caused by ply drops. The ESN laminate had an exterior zero degree layer as the butt joint, while the ESO laminate had an interior $\pm 45^\circ$ layer as the butt-joint. The actual lay-up in the ESN and ESO laminates was $[0/\pm 45/0]_s$.

The ESP laminate had the lay-up, $[0/\pm 45^*/\pm 45^*/\pm 45/0/(0/\pm 45/0)_2]$, to evaluate the

effect of dropping $\pm 45^\circ$ layers. In this laminate the thickness was tapered 18%, with no zero degree layers being dropped. The ESQ laminate had the same lay-up as the ESH laminate, two interior zero degree ply drops, but the fabric being used for the zero layers was the warp unidirectional woven A130. The last laminate is ESR, which had the lay-up $[0/\pm 45/0/\pm 45^*/\pm 45^*/0/\pm 45/0]$. This looked at the effect of dropping multiple $\pm 45^\circ$ layers in a thinner laminate. No zero degree layers were dropped, and the thickness was tapered 25%.

Additional coupons investigated the possibility of suppressing delamination by adding to or tailoring the laminate properties. The first configuration used the ESA laminate as a basis for comparison, and a second configuration used the ESB laminate as a basis. For the JKA coupons, random mat fabric was included between the ply drop and the first continuous zero layer. Random mat was not used in the internal ply configuration case. A second modification is called "feathering." In this case, alternating tows were pulled one half inch past the adjacent tows to provide a less defined delamination site. This modification along with "Z-Spiking" can be seen in Figure 6.

Material Preparation

The various E-glass/polyester materials used in this thesis were all manufactured by RTM (Resin Transfer Molding), which consisted of a peristaltic pump forcing the resin into a closed, vented mold containing the reinforcing layers[48]. To incorporate ply drops into the manufacturing process, the following procedure was used to prepare the mold. First the mold was coated with a mold release (Frekote 700- NC), air dried, then the individual fabric layers were placed in the mold. The lay-up of a laminate with ply

drops is shown in Figure 7. Ply drop layers (4) were cut to shorter lengths and placed in the desired position along with the continuous layers (3). Fluoro-Peel release film (2) was added to the laminate to accomplish the thickness reduction in the desired area, with

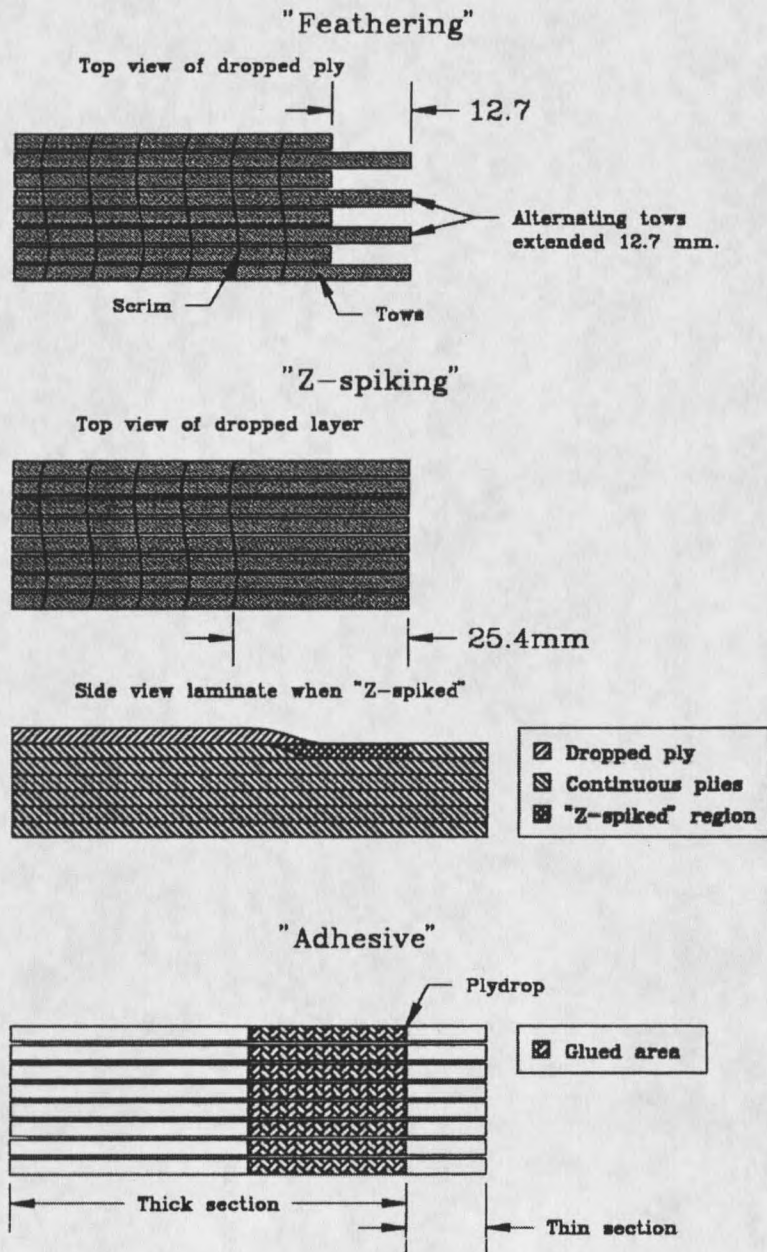


Figure 6. Different delamination prevention techniques.

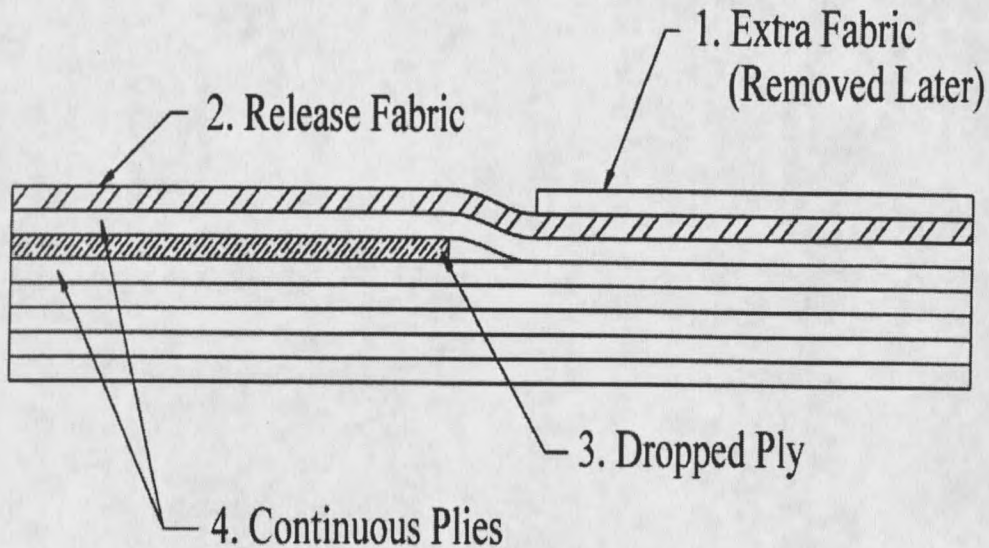


Figure 7. Lay-up of laminate with ply drops in mold

fabric layers (1) added over the release film so that the fiber content was the same in the thin and thick sections. When the resin was injected into the mold, the porosity of the sample was low (<1%), except for the resin rich region in front of a ply drop which was often observed to have some localized higher porosity.

Fabrics

The E-glass fabrics used in these experiments were from Owens-Corning Fabrics (formerly Knytex). Three different types of fabric were used in these experiments. Wind turbine blades, because they are long and thin need to use a high percentage of continuous warp unidirectional fabric oriented with fibers in the length (0°) direction to give them stiffness. They also usually incorporate $\pm 45^\circ$ fabrics to control twisting. Unidirectional fabrics, from Owens-Corning, are available in either the warp or the weft direction. Warp fabric means that the individual tows of glass fibers are oriented parallel to the long

direction of the fabric when it is rolled up; conversely, weft fabrics have the unidirectional tows oriented so they are perpendicular to the length of the roll, which is generally only 1.3 meters wide. D155 fabric is a unidirectional fabric which weighs approximately 526 grams/ m². The D155 fabric is available in the weft direction only, and while the properties are good, the current manufacturing lengths makes it unsuitable for structures longer than 1.3 meters. The second type of unidirectional fabric used in this thesis is A130. This fabric is a woven warp unidirectional fabric which has good tensile properties, but because of the curves introduced from large thermoplastic beads connecting the tows, creating the weave, the compressive properties are significantly less than the D155 properties [49]. Finally the $\pm 45^\circ$ fabric layers involve the DB120 fabric, the DB representing double bias fabric of 407 grams/m².

The resin used in these experiments was CoRezyne 63-AX-051, an unsaturated orthophthalic polyester, manufactured by Interplastic Corporation. This resin was combined with methyl ethyl ketone peroxide (MEKP), 2% by volume, to catalyze the cross-linking reaction. Curing of the materials was at ambient conditions, followed by two hours at 60°C

Specimen Preparation

After the plates had been left to cure for at least five hours, they were removed from the mold. The edges were trimmed off to eliminate any edge anomalies. All specimens were cut using a water-cooled diamond saw. The coupon edges were then polished in sequential steps down to 400 grit emery paper from Buehler. This helps to suppress, but not eliminate, edge generated delamination. For coupons run to more than

10^5 cycles, fiberglass tabs were bonded onto the ends with Hysol EA 9309.2NA adhesive. The coupons were then post-cured a second time at 60 °C for two hours. Tensile coupons were 20 cm long by 2.5 cm wide with a gage section of 13 cm. Compressive coupons were 10 cm long by 2.5 cm wide with a gage section of 5 cm.

All coupons were tested for the fiber content using a matrix burn-off method described under ASTM D 2584. The only deviation from the ASTM standard was in the amount of material used in the burn off test, 15 to 20 grams rather than the prescribed 5 grams.

Test Facility and Development

All of the coupons were tested using an Instron 8501 servo-hydraulic machine. This machine allowed maximum and minimum peak loadings to be accurately maintained while varying the loading wave forms and counting the number of cycles applied to the specimen. The specimens were clamped into the Instron using hydraulic grips. The amount of pressure used to clamp the specimens was varied according to the maximum stress experienced by the specimen, to prevent coupon crushing. If, during the course of the test, the grip hydraulic pressure gauges fluctuated, which could indicate sample slipping, the test would be stopped and additional pressure would be added to the grips. This method was used to avoid over-clamping the specimens and causing excessive gripping or tab failures.

An extensometer (Instron 2620-525) was used to determine strains for calculation of the initial modulus. The extensometer was attached to the edge of the coupon via rubber bands. In all cases the initial longitudinal elastic modulus, E_x , was

measured on the thin section of the coupon by taking a least squares fit of at least five equally spaced load intervals. The modulus of the thin section then provided a basis for calculating the maximum running strain for a given stress.

A minimum of three static tests were performed to obtain an accurate ultimate tensile strength for each laminate. These static tests were performed under displacement control, with a displacement rate of 12.7 mm/sec. Fatigue tests used a sine-wave cyclic waveform with the testing machine in load control. The first coupons were set to run at a maximum stress of approximately 60% of the ultimate stress, with a minimum stress of 10% of the maximum stress, giving an R value of 0.1 ($R = \text{minimum stress} / \text{maximum stress}$). After these coupons failed, a best fit line through the two points was used to predict the approximate lifetime of coupons being run at different stress levels. All test coupons were run at frequencies where the coupon temperature did not rise more than 5 °C above room temperature. A fan was placed approximately one meter away to provide additional cooling of the coupons. Fatigue tests were either performed until failure, which was defined as the inability of the coupons to carry the maximum load, or until delamination at the ply drop extended along the entire length of the coupon and into the grips.

DCB and ENF test specimens

These experiments were run to characterize the pure Mode I and Mode II delamination resistance, G_{Ic} and G_{IIc} . These lay-ups were $[0]_{10}$, $[(0)_5/\pm 45/(0)_4]$, and $[\pm 45]_{10}$. Figure 8 shows typical DCB and ENF specimens. The main requirement for double cantilever beam (DCB) specimens is to ensure that delamination propagates along the mid-plane. This was accomplished by inserting a 25 mm wide piece of Fluoro-Peel release fabric between the layers of interest to form the starter crack. Once the mold had

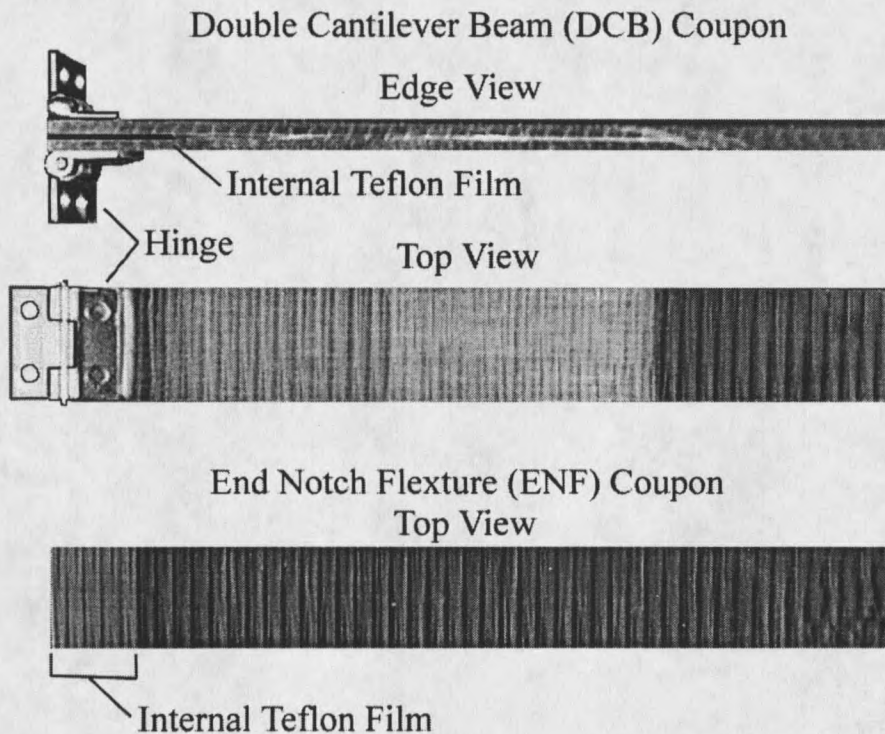


Figure 8. DCB and ENF specimens

time to cure the plate was cut into test coupons with dimensions of 25 mm wide by 200 mm long, and a nominal thickness of 5 mm. A starter crack, 3 mm long, was introduced

into the coupons, to bypass the resin-rich area ahead of the release fabric, with a flat head screwdriver. The area where the hinges were to be mounted for loading was then sanded to remove any release agent from the molding process. Typical piano stock hinges were then mounted to the coupon ends using Hysol EA 9309.2NA adhesive. The end notch flexure (ENF) specimens had the same dimensions as the DCB specimens, but with no hinges.

CHAPTER 4

RESULTS AND DISCUSSION

This chapter is divided into four sections. The first section presents results for the delamination resistance of various laminates, where the delamination was allowed to progress over the entire specimen length. Comparison between various ply drop combinations are made in terms of delamination growth rates as well as initiation and arrest. The second section looks at the influence of ply drops on the fatigue lifetime of the laminates, including design knockdown factors. Appendix A contains the fiber content, elastic modulus, maximum running stress and the number of cycles to which each coupon was fatigued. Appendix B contains the delamination length versus cycles for all of the coupons tested in the first section. The third section presents results for composite I-beams containing ply drops, comparing results in these structural components with coupon results. The last section presents basic results for critical strain energy release rates in Modes I and II delamination using double cantilever beam and end notch flexure coupons, respectively.

Delamination Study

Effect of Ply Drop Location

Table 1 lists details of laminates ESA, ESB, and ESC, each of which contained a single 0° ply drop. The ESA laminate has a single exterior 0° ply drop. Static tensile tests

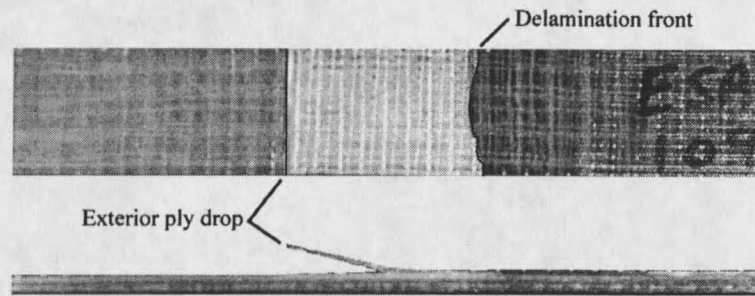


Figure 9. Delamination of exterior zero degree ply drop.

produced delamination of the dropped ply over the entire specimen free length, as seen in Figure 9, followed by a brooming type of failure of the remaining cross-section, shown in Figure 10. This type of dramatic failure is typical for all laminates tested statically, and Figure 10 is also typical of laminates without ply drops.

The ESA laminate was tested in tensile fatigue at various maximum stress levels at an R value of 0.1 to characterize the fatigue crack growth of the delamination. Figure

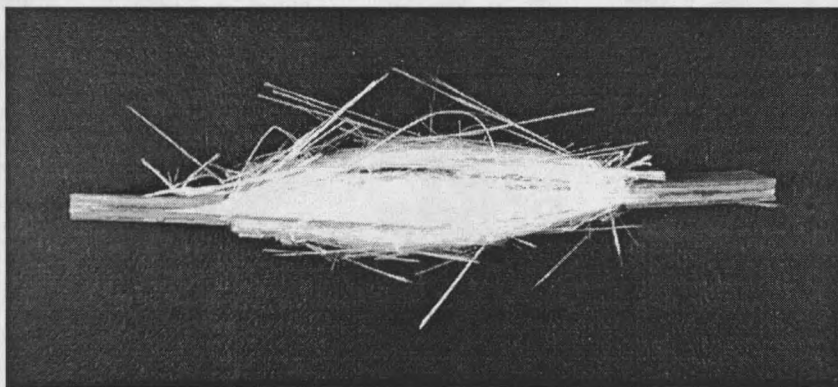


Figure 10. Typical static failure of laminate with ply drop.

11 shows results for delamination length versus cycles at three maximum stress levels.

These are results for typical individual tests; results for all tests are given in Appendix B.

These coupons delaminated uniformly across the coupon width and along the gage length.

Measuring the length of the delamination was straight-forward, because the initially

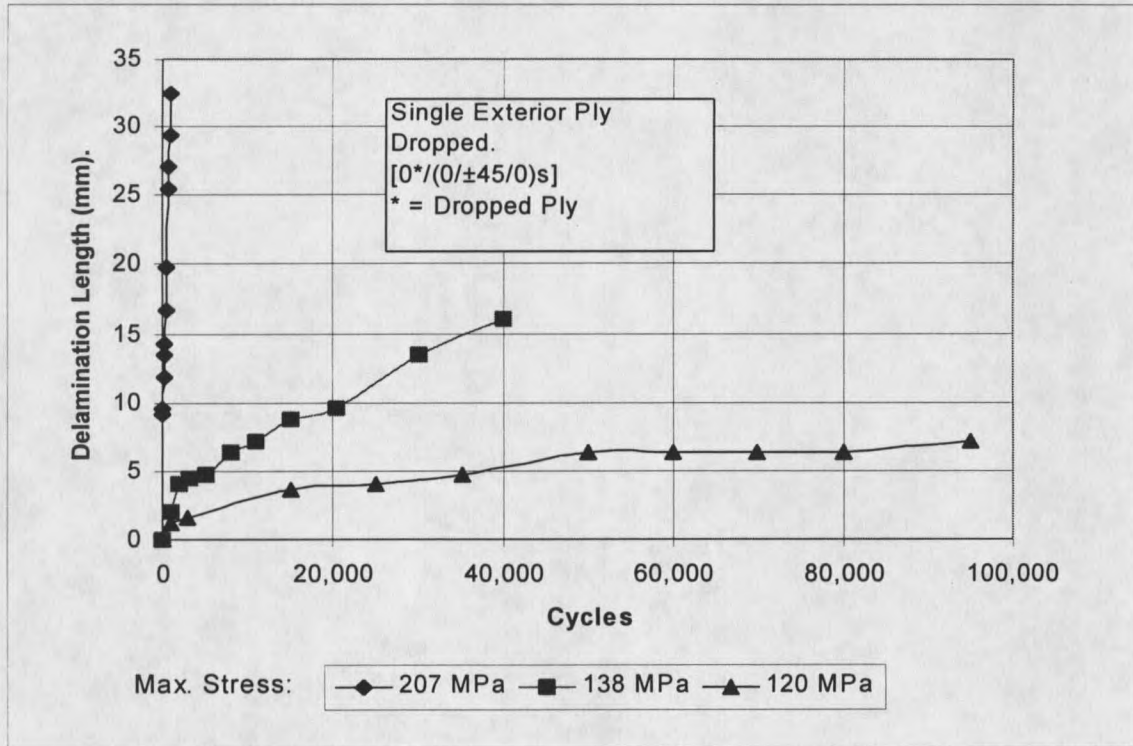
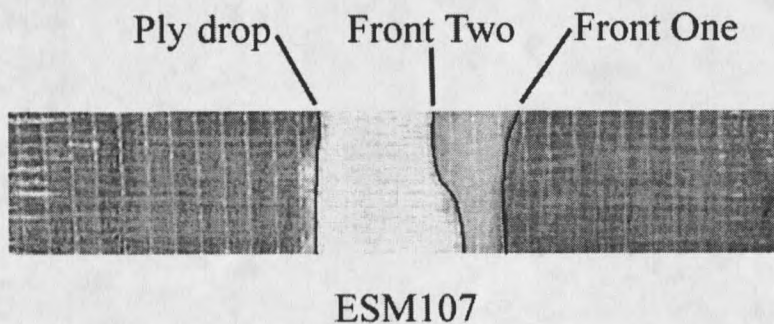


Figure 11. Delamination length vs. cycles for ESA laminate, $R = 0.1$, Exterior 0° Ply Dropped.



ESM107

Figure 12. Delamination at an interior ply drop showing two delamination fronts.

translucent coupons became opaque due to the delamination. In Figure 9, an ESA coupon is shown with the exterior 0° delaminated. This type of delamination is typical for all of the laminates with exterior ply drops. The coupons showed no other signs of fatigue damage. Unlike laminates with an exterior ply drop, interior ply drops developed two different delamination fronts. These two delamination fronts can be seen in Figure 12 for the ESB laminate $[0/0^*/\pm 45/0/0/\pm 45/0]$. The crack initially started in between the $+45^\circ$ and -45° plies under the ply drop, labeled Front One in the Figure 12. The delamination then propagated along the length ahead of the second delamination front, labeled Front

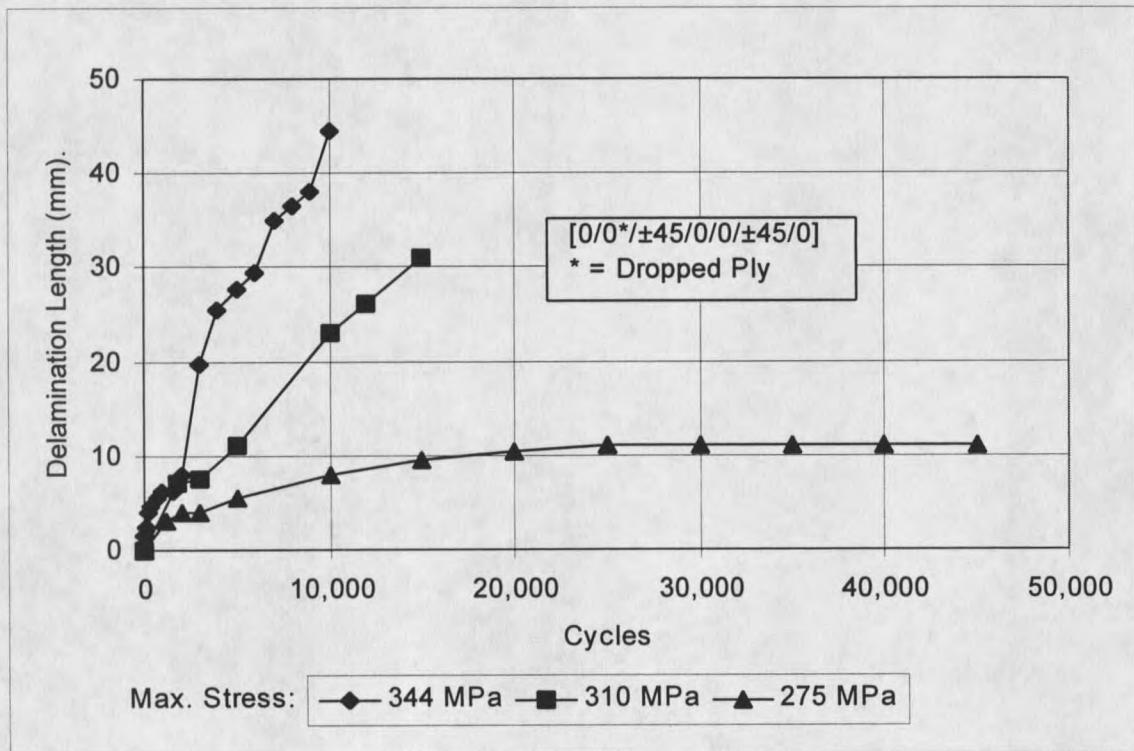


Figure 13. Delamination length vs. cycles for ESB (Single interior 0° ply drop) laminate, $R=0.1$.

Two, which developed between the exterior zero ply and the ply drop layer. For the interior ply drop, in the ESB laminate, delamination required about twice as high a

maximum stress level as for the ESA laminate, apparently due to the two shear surfaces, as discussed later. The delamination rate for various stress levels for both the ESB and ESC laminates can be seen in Figures 13 and 14. The ESC laminate, with a central ply drop, showed a slightly higher delamination resistance than ESB.

Table 2 provides an approximate measure of delamination resistance based on the delamination test results. The Table rates delamination resistance for different laminates in terms of the maximum strain under tensile fatigue loading to produce a one-inch long

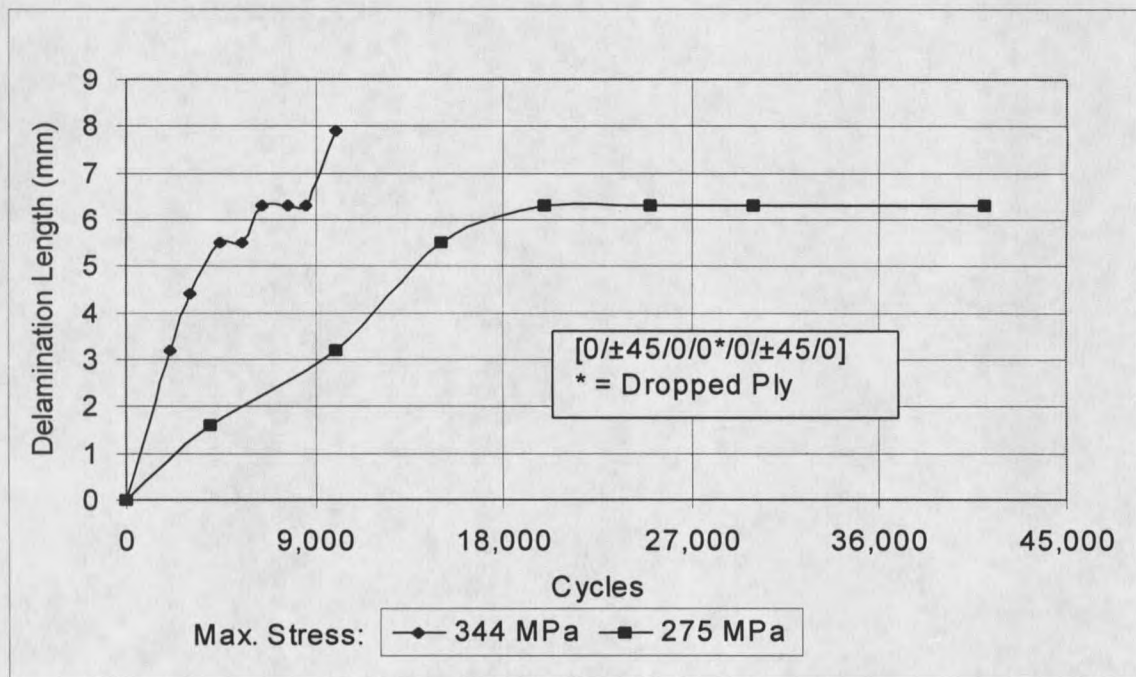


Figure 14. Delamination length vs. cycles for ESC (Single center interior 0° ply drop) laminate, $R=0.1$.

delamination in 10^5 cycles. The ESA laminate with an exterior ply drop required only 0.6% maximum strain in fatigue to produce a 25 mm delamination in 10^5 cycles, while the ESB and ESC laminates required about 1.1% maximum strain. The stresses and strains in each case are the values measured and calculated for the thin cross-section side of the ply drop. The arrest strain values are obtained from the highest stress where the

Table 3. Comparison of delamination resistance of different ply drop configurations.

Laminate	Lay-up	% Strain for 25.4 mm delamination in 10 ⁵ cycles	Arrest % strain ¹	Threshold % strain ²
ESA	[0*/(0/±45/0) _s]	0.6	0.5	0.4
ESB	[0/0*/±45/0/0/±45/0]	1.1	1.1	0.8
ESC	[0/±45/0/0*/0/±45/0]	1.1	1.1	0.8
ESE	[0*/(0/±45/0) ₃]	0.6	0.4	0.4
ESF	[0/0*/±45/0/(0/±45/0) ₂]	1.0	1.0	0.7
ESG	[0*/0*/(0/±45/0) ₃]	0.4	--	--
ESH	[0/0*/0*/±45/0/(0/±45/0) ₂]	0.7	0.6	0.5
ESI	[0/0*/0*/±45/0/0/±45/0]	1.1 ^A	1.0	0.7
ESJ	[0*/(0/±45/0) _s] "Z-Spiked"	0.8	--	--
ESK	[0*/(0/±45/0) _s] Hysol EA 9309.2NA	0.7	--	--
ESM	[0/0*/±45/0/0/±45/0] Hysol EA 9309.2NA	1.1 ^B	--	--

¹- no further growth over most of the 10⁵ cycles

²- no delamination after at least 10⁵ cycles.

Fabrics: 0°: D155; ±45°: DB120 except as noted

Laminates ESO, ESR and ESP not shown, ±45° layers did not delaminate.

^A- Same as ESB, except multiple ply drops.

^B- No delamination; however, failure of coupon occurred at ply drop.

delamination arrested after 10^5 cycles. The threshold strain values are obtained from the highest stress where no delamination had formed after 10^5 cycles. These results are limited to the 10^5 cycle range, and could vary at high cycles.

Effects of laminate thickness and multiple ply drops at the same position

Two significant parameters in dropping plies are the percentage of the total thickness (and total 0° plies) which are dropped, and the number of plies which are dropped at the same position. These parameters were explored with laminates ESD through ESH. Laminate ESD had two interior 0° ply drops, while maintaining the same basic lay-up as the thin sections of the ESA, ESB and ESC laminates, without adding additional 0° plies to be dropped. This resulted in a 33 percent drop in thickness (a 50% drop in the percent 0° plies), whereas the ESA, ESB and ESC laminates were only tapered 14 percent, with 20% of 0° plies dropped. This interior ply drop did delaminate when statically loaded to failure, but no delamination occurred when the coupon was fatigued. The laminate simply broke through the thickness at the ply drop. The difference can also be seen in the moduli of the thick and thin sections, 22 GPa versus 15 GPa, respectively, resulting from a higher percent of 45° material in the thin section (Table 1). This bounds the practical range of thickness taper that can be used successfully in a design. Having too much taper can prevent delamination, but only because the thin section can only support very low loads. Only two coupons were tested since no delamination occurred prior to tensile failure.

The ESE and ESF laminates

The ESE and ESF laminates incorporated a single 0° ply drop into a base laminate that was thicker than the ESA laminate. The percent thickness change in these laminates was reduced to 10% as compared to the 14% for the ESA laminate. The ESE laminate had an exterior ply drop while the ESF laminate had an interior ply drop. The delamination rate was slightly lower for the ESE laminate than for the ESA laminate (Figure 17), but the strain to produce a 25 mm delamination in 10^5 cycles was about the same, 0.6% (Table 2). The ESF laminate also had a slightly slower delamination rate than the ESB laminate, but the strain value in Table 2 was slightly lower at 1.0% for ESF versus 1.1% strain for ESB. The delamination mode of both of these laminates was very similar to their thinner counterparts.

The ESG and ESH laminates were also thicker in cross-section, plus, in an attempt to simulate a manufacturing situation, two plies were dropped instead of one. The ESG laminate contained two dropped plies on the outside while the ESH laminate contained two dropped plies in the interior (Table 1). In both cases these configurations behaved poorly compared with their single ply drop counterparts. During testing of the ESH laminate, the resin rich area ahead of the ply drop was observed to crack extensively during the fatigue test. When the coupon was at the maximum stress of the fatigue cycle, fracture and fragmentation in the resin pocket occurred. No matrix material was left ahead of the ply drop after the initial cycles. This is illustrated in the Figure 15.

The ESG laminate, with a double external ply drop, delaminated more easily than

a single ply drop on the outside. The percent strain for a one-inch delamination in 10^5 cycles for ESG and ESH were 0.4% and 0.7%, respectively. These are significantly lower than the values for their counterparts single-ply-drop cases, ESE and ESF at 0.6% and 1.0% strain, respectively (Table 2). A comparison of laminates having internal ply drops is presented in Figure 16. As noted, the ESH laminate with two interior ply drops had the highest delamination rate. (The ESK laminate is discussed later).

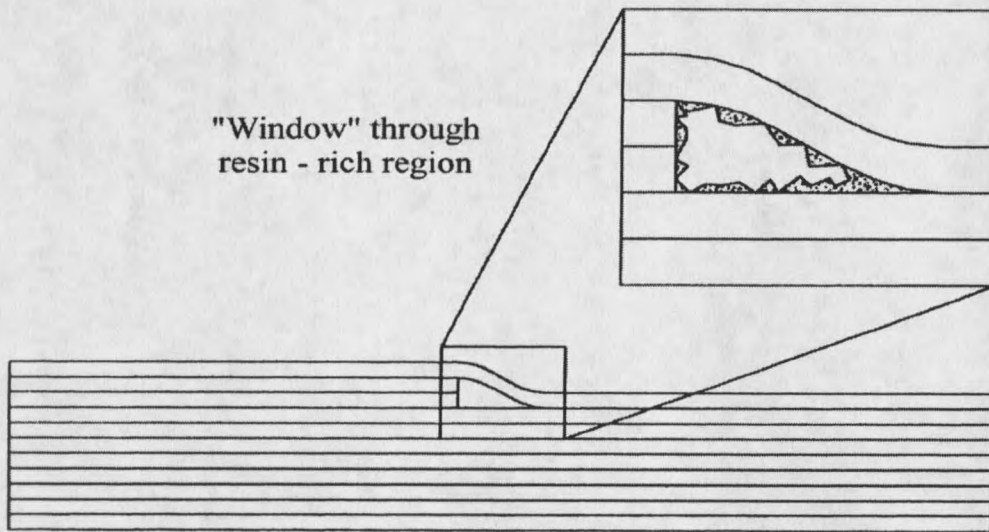


Figure 15. Illustration of resin rich region in ESH laminate.

Effect of Ply Drop Spacing

The ESI laminate was constructed to look at the effect of multiple individual ply drops with spacing ranging from 13 to 48 mm, and are compared with the ESB laminate having the same ply configuration and a single ply drop. The results for the various cases in Figure 17 are scattered with no clear effect of spacing. The closest spacing, 12 mm, gives results which are essentially the same as for ESB laminate with a single, interior ply

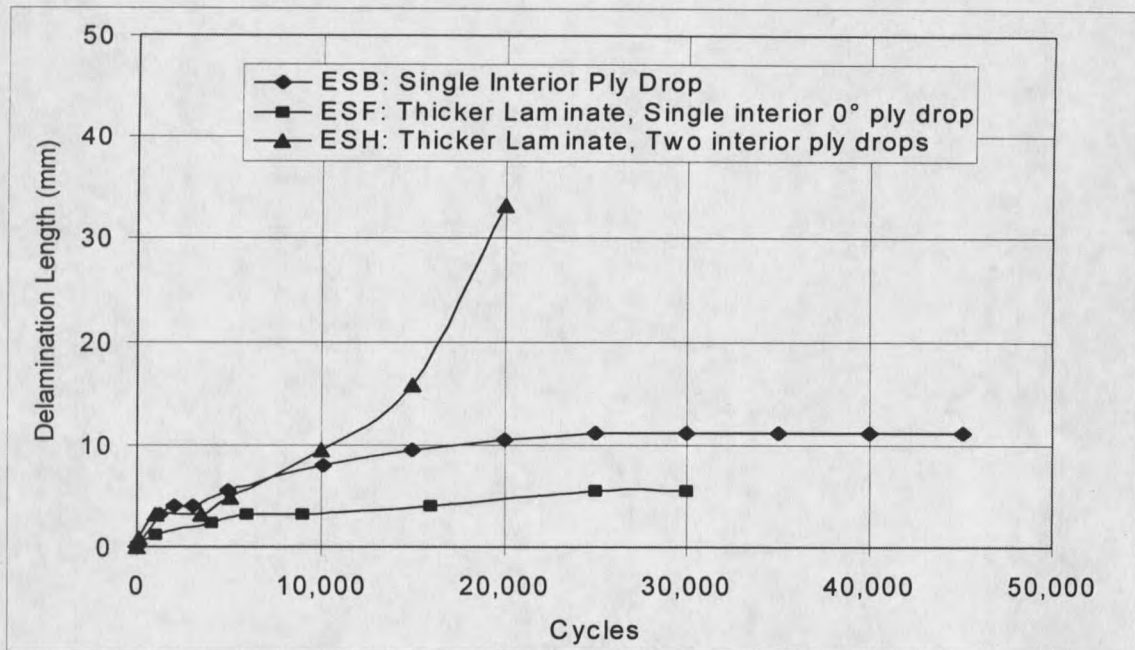


Figure 16. Delamination length vs. cycles for laminates ESB, ESH, ESF (all interior ply drops) at a maximum running stress of 275 MPa, R=0.1

drop. However, if the two delaminations merge together, then a single system is created which might propagate like the case with two dropped plies at the same location.

Complete data to explore this question were not generated, but typical coupons containing multiple ply drops with delaminations can be seen in Figure 18. All the coupons were run at the same stress level, 275 MPa, with $R = 0.1$. A coupon with ply drops too close together can be seen at the top of Figure 18 right before both ply drops delaminated together. In the lower two coupons the delamination has arrested after some crack propagation, prior to the delamination combining into a single system.

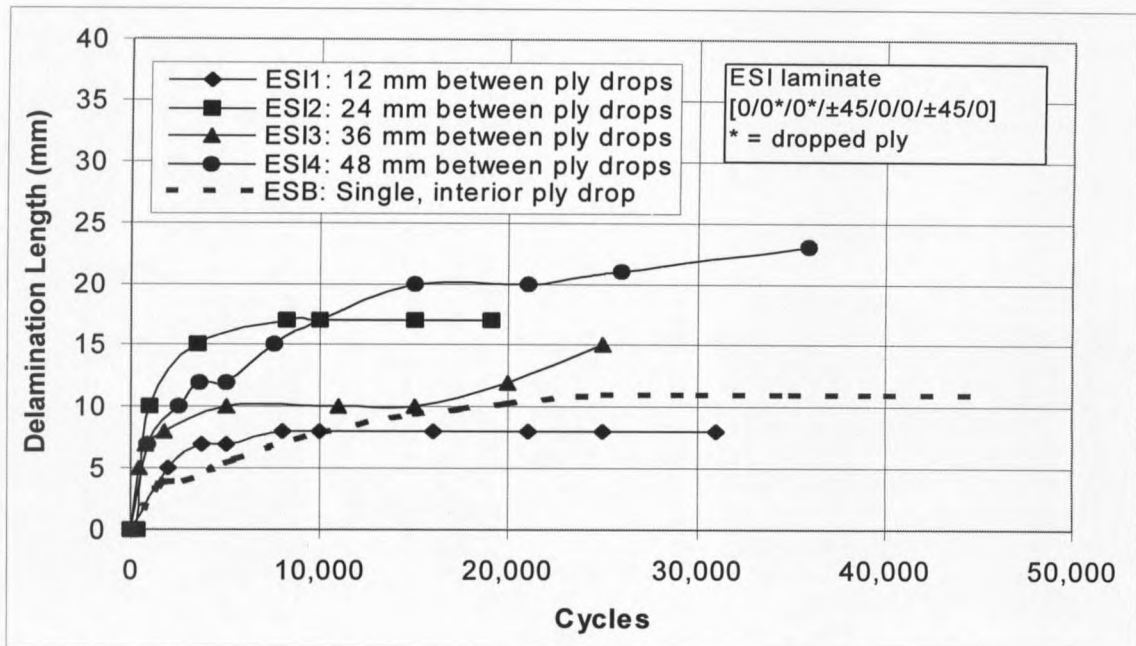


Figure 17. Effect of different spacing between ply drops, $R=0.1$, ESI laminate (Two 0° ply drops) at 276 MPa.

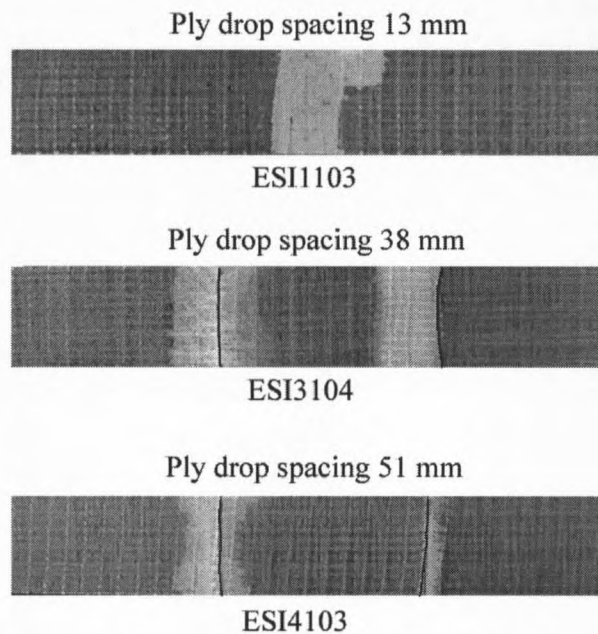


Figure 18. ESI coupons run at 276 MPa, $R=0.1$.

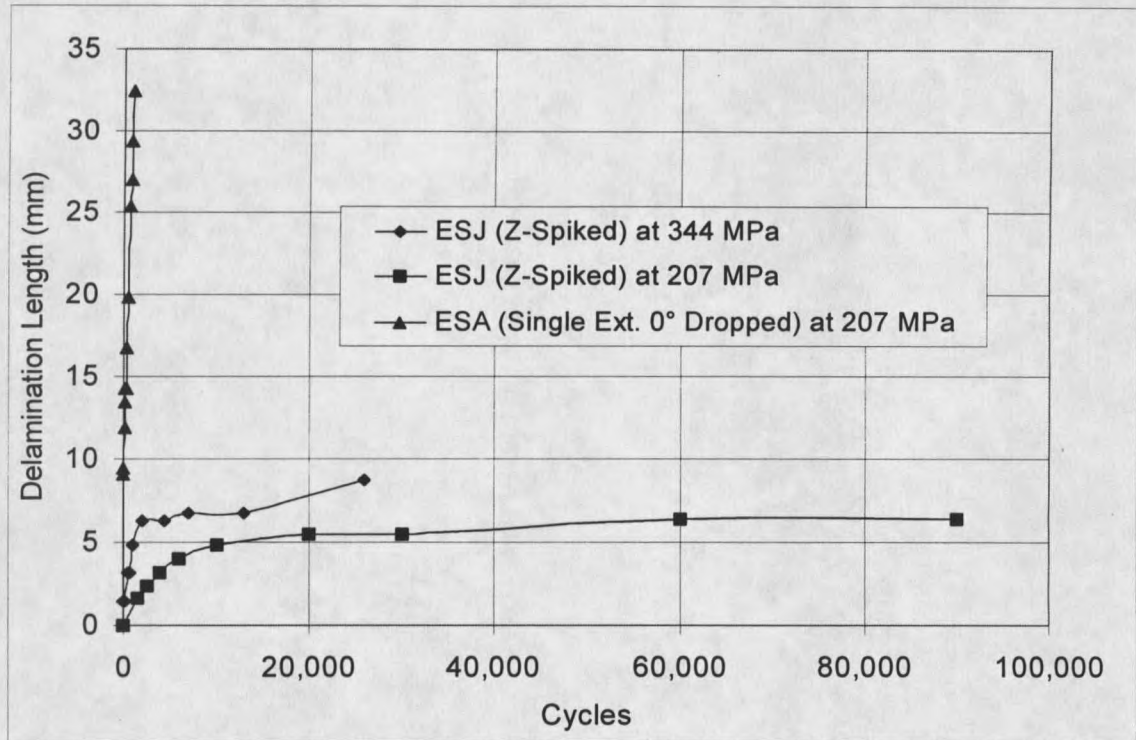


Figure 19. Delamination length vs. cycles for ESJ “Z-Spiked” laminate compared to ESA (Single, exterior 0° ply drop) laminate, R= 0.1.

Effects of “Z-Spiking”

The ESJ laminate with “Z-Spiking” is not shown in Figure 19, which compared laminates with exterior ply drops at a maximum stress of 138 MPa, because there was no delamination until more than 200,000 cycles. Delamination at higher stresses in the “Z-Spiked” laminate initiated locally around the tows and then proceeded into the ply drop. The delamination initiation took longer than for a normal exterior ply drop.

Delamination rates at various stress levels for the “Z-Spiked” laminate can be seen in Figure 19 compared with data for the ESA laminate. At the lowest stress level shown using the “Z-Spiked” configuration (207 MPa), the ESA laminate completely delaminated rapidly, but the “Z-Spiked” laminate had reached a level where the

delamination arrested. The laminates with interior ply drops and “Z-Spiking” showed a definite improvement in delamination resistance over laminates that were constructed normally. The ESM laminate, with a “Z-Spiked” internal ply drop, was not successful in preventing delamination. A delamination immediately formed in the area where the $\pm 45^\circ$

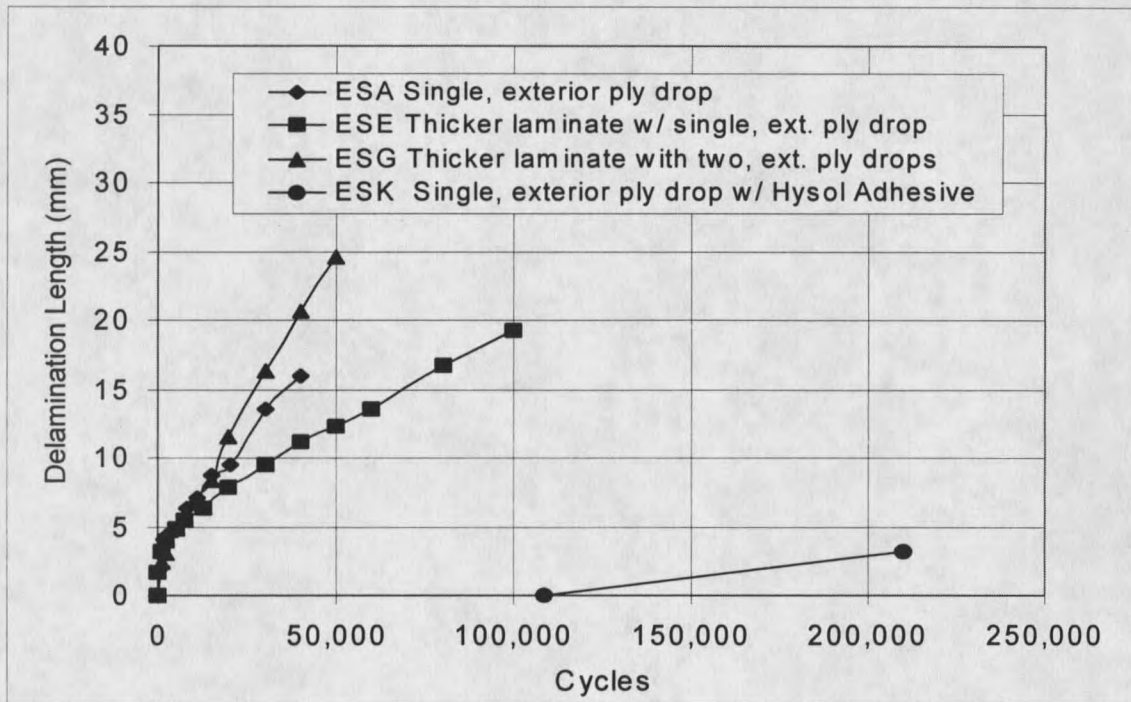


Figure 20. Delamination length vs. cycles for laminates ESA, ESK, ESG, ESE (all exterior ply drops) at a max. running stress of 138 MPa, R=0.1.

layer was completely severed to allow the ply drop to be inserted. The delamination then propagated at the same rate as a typical ESB laminate.

Effect of Tough Adhesive at Ply Drop

The ESK and ESL laminates had single ply drops where the ply drop area was impregnated with Hysol EA9309.2NA epoxy adhesive prior to resin impregnation. In Figure 20, the ESK laminate with the Hysol adhesive is compared with three other laminates that incorporated an exterior ply drop. The ESK laminate showed a significant

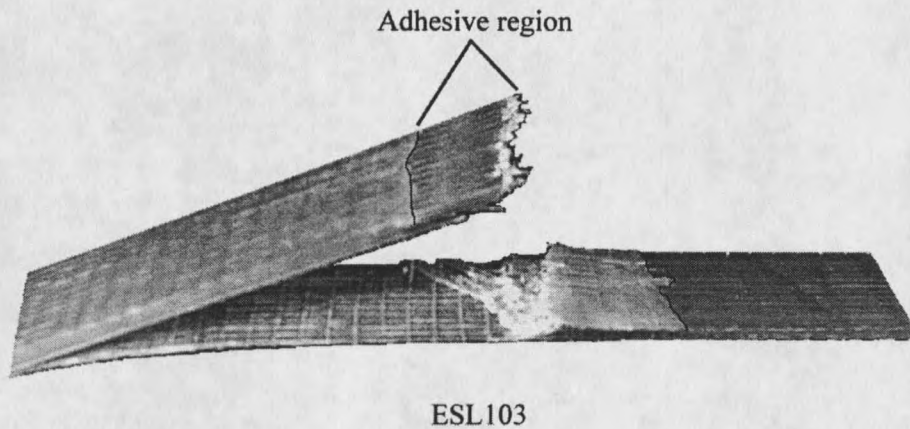


Figure 21. ESL laminate in tension at the ply drop (Interior 0° ply drop with Hysol adhesive) failed at 276 MPa.

improvement over the other configurations tested. The delamination in the ESK laminate did not initiate until the other laminates had completely delaminated. The delamination did not initiate in the adhesive, but at the point right behind the adhesive, in the thicker section. Once the crack had propagated to the grip, the adhesive failed, totally separating the plies. The ESL laminate, with an interior ply drop with adhesive, showed no visible delamination prior to coupon failure. A typical failure can be seen in Figure 21. The region where the adhesive was allowed to cure did not delaminate prior to total laminate failure. Failure occurred near the ply drop location, apparently due to the stress concentration from the ply drop. This type of prevention technique provided significant delamination prevention, while not reducing the life of the coupon when compared with the ESB laminate at the same number of cycles, as discussed later.

Effect of Butt-Joints

The ESN and ESO laminates were used to investigate the effect of butt-joints on

the delamination properties of typical laminates used in this thesis. The ESN laminate contained an exterior 0° butt-joint. This had the same effect as dropping a ply, as the ply delaminated at the same rate as for the ESA laminate. However, the ESO laminate contained an interior $\pm 45^\circ$ layer butt-joint. The $\pm 45^\circ$ layer did not delaminate and caused no damage which influenced the lifetime of the coupon. This suggests that dropping $\pm 45^\circ$ layers makes for a less delamination critical design. This is not surprising since zero degree layers carry the majority of the load and have the greatest influence on stiffness. However, dropping $\pm 45^\circ$ layers can only be used to a limited extent, since they are not present in great numbers in this class of laminates.

Effects of $\pm 45^\circ$ Ply Drops

To confirm the effect of dropping $\pm 45^\circ$ degree layers on delamination rate, the ESR laminate was laid up similar to the ESC laminate. However, instead of incorporating two interior 0° ply drops, the ESR laminate incorporates two $\pm 45^\circ$ ply drops along the centerline. This laminate showed no signs of delamination into the thick section as did all the other laminates, as the delamination actually propagated into the thin section. This delamination may have been artificially influenced by the high degree of tapering, 25% of the thickness, which caused a severe shape change.

To get a better estimation of the influence of $\pm 45^\circ$ layer ply drops, the ESP laminate was manufactured with two $\pm 45^\circ$ ply drops (four total plies). The laminate showed no signs of delamination, even after 300,000 cycles at maximum stress of 276 MPa, whereas the ESH laminate, with two interior 0° layers, had delaminated. However, after this many cycles the coupons had premature end failures. This laminate shows

results that are consistent with the laminate containing the $\pm 45^\circ$ butt-joint. The $\pm 45^\circ$ layers are much more compliant than 0° layers and are less prone to delamination at ply drops.

Effect of A130 warp unidirectional fabric

The ESQ laminate used the same laminate lay-up as the ESH laminate, but made use of the A130 unidirectional woven warp direction fabric in place of the D155 weft fabric used in other laminates. The delamination could not be measured with any consistency from coupon to coupon. The A130 fabric is constructed of unidirectional strands woven around a transverse thermoplastic bead every 25 to 30 mm. The delamination would propagate from one bead to the next and then arrest. After continued fatigue the delamination would jump to the next bead. However, the A130 fabric overall showed less delamination resistance than the D155 fabric, with the delamination propagating unstably between beads. A typical example of this is that at 310 MPa level, a laminate using the A130 fabric would delaminate to the grips in under one thousand cycles, whereas a laminate using the D155 fabric would not delaminate that far until after 30,000 cycles.

Other attempts to prevent delamination

The JKA "Feathered" and "Random" laminates used the ESA laminate with an exterior ply drop as a model to incorporate delamination suppression techniques, in addition to the "Z-Spiked" and adhesively bonded ply drops. The results in Figure 22 show that the random mat had no effect on the delamination rate, while incorporating feathering in the laminate is very successful at retarding delamination. The delamination of the JKA "Feathered" laminate began at the tip of the tows that had been pulled out so they extended beyond the fabric edge, and propagated along those tows until it reached

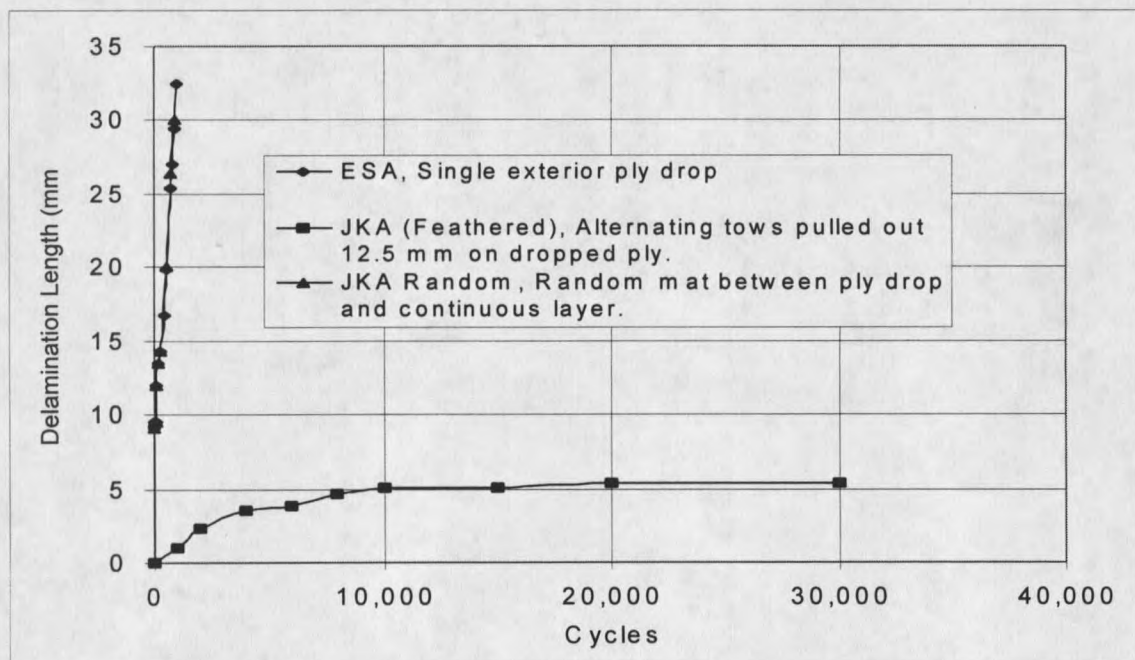


Figure 22. Delamination length vs. cycles for ESA, JKA "Feathered" and JKA random laminates at a maximum running stress of 207 MPa, R=0.1.

the tows which were not pulled out. The delamination can be seen propagating along the pulled out tows in Figure 23. The JKB "Feathered" used the same scheme to prevent



Delamination initiating along tows that are pulled out

Figure 23. Delamination initiating along tows pulled out.

delamination in an internal ply drop laminate. The delamination progressed the same way as with the JKA "Feathered". The JKB "Feathered" delamination rate is compared to a standard ESB laminate in Figure 24. The "feathering" has a significant effect on reducing the delamination length.

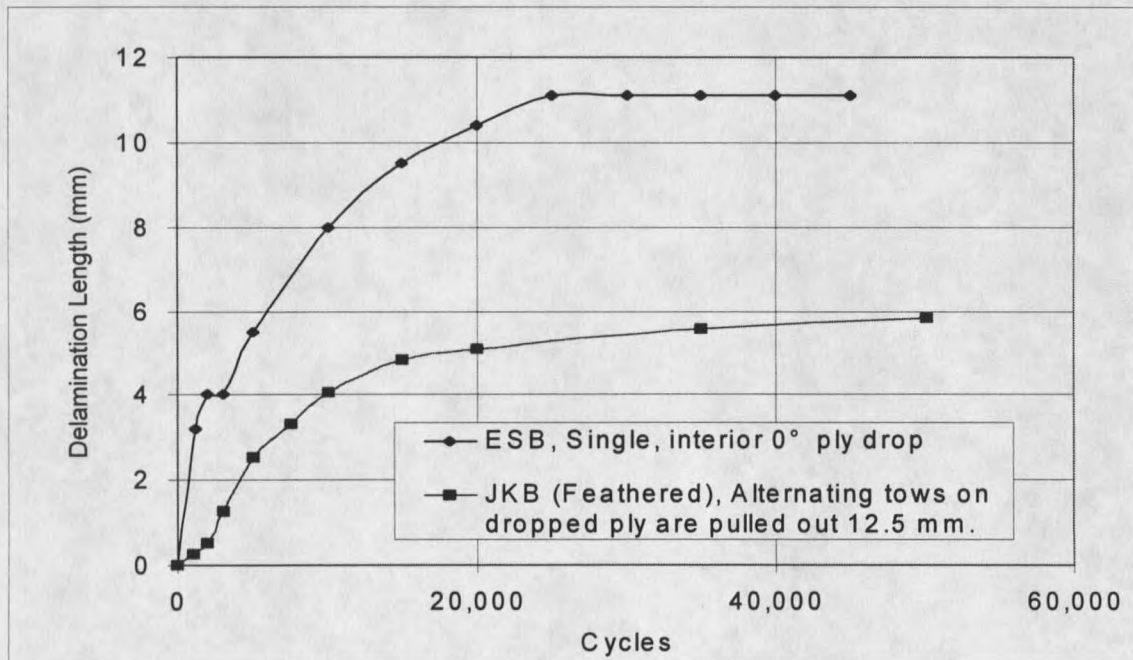


Figure 24. Delamination length vs. cycles for ESB and JKB "Feathered" at a maximum running stress of 275 MPa, R=0.1.

Repairing Delaminated Samples

If exterior ply drops are to be used in a design and an overload condition takes place, it would be desirable to repair the delamination. Two epoxy adhesives, Hysol EA 9309.2NA and Hysol EA 9412, were used to repair the delamination. After the initial test was run on an ESA laminate, causing delamination, the adhesive was injected into the delamination and a C-clamp was applied to the specimen until the adhesive had cured. The specimen was then retested at the same stress level and the delamination rate was

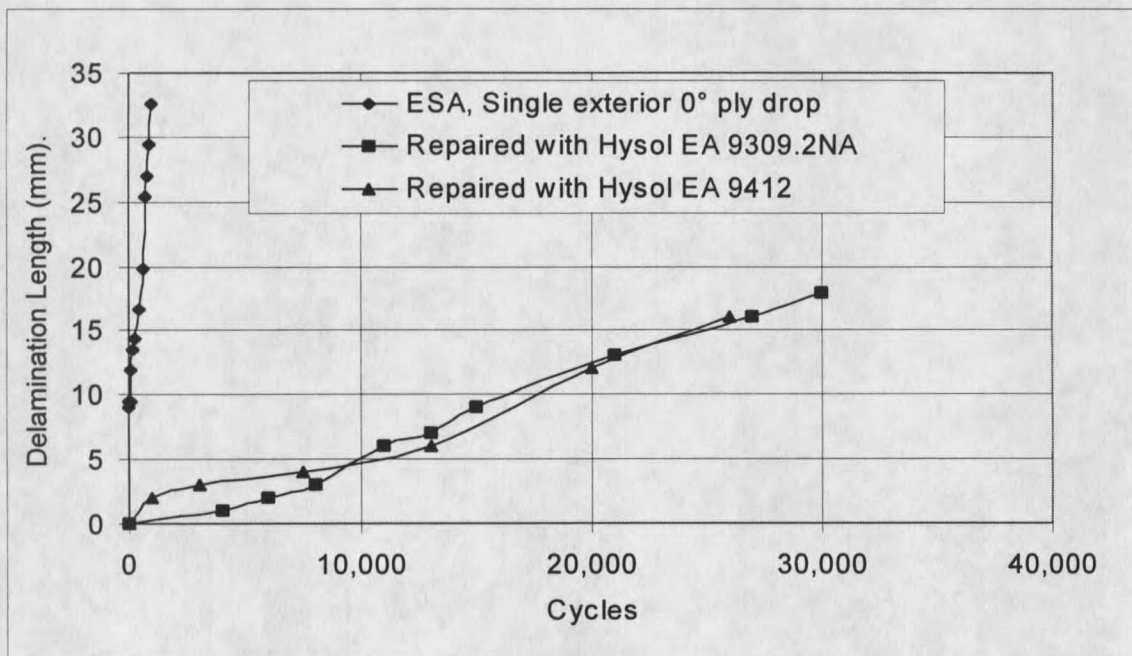


Figure 25. Delamination length vs. cycles at 207 MPa, R=0.1, initial ESA laminate compared to repaired ESA laminate.

compared to the original rate, which can be seen in Figure 25. From Figure 25, the two adhesives had a similar delamination rate and provided a significant reduction in delamination rate compared with the original laminate.

So far the only attempts to repair delamination have involved exterior ply drops, since interior ply drops present an access problem. One possible method of repair would be to drill a hole into the laminate that is smaller than the critical flaw size and draw a vacuum around the hole. This would draw the repair adhesive into the delamination and possibly extend the lifetime of the component. (This has not yet been demonstrated.)

Comparing different laminates

In order to make this work useful to a designer needing to incorporate ply drops into a design, Table 2 compares the various laminates, by listing the percent strain needed to cause a 25 mm delamination at 10^5 cycles. By knowing the apparent penalty for using different ply drop configurations, more efficient designs can be developed. For example, by using an exterior ply drop instead of an interior ply drop, there would be an 83% reduction in the strain-carrying capability of the laminate. Another example would be if two plies are dropped on top of one another instead of the plies being distributed along the length, there would be a 57% reduction in the strain-carrying capability of the laminate. Similar conclusions are evident for the strains to arrest a delamination and for the threshold strain to initiate a delamination, also listed in Table 2.

Effect of Ply Drops on Lifetime

In the previous sections, different lay-ups were tested in relatively short fatigue tests to determine the rate of delamination. This section describes a study of the ESB and ESH configurations at extended fatigue cycling, in terms of the effect of ply drops on total coupon lifetime. The ESH laminate consisted of the lay-up [0/0*/0*/±45/0/0/±45/0/0/±45/0], where the asterisk plies are being dropped. The ESB laminate, with a single ply drop, had a lower delamination rate than the ESH laminate in the delamination fatigue tests.

Fiber Volume Content Effect

The results are represented in terms of conventional S-N fatigue data sets for control and ply drop cases. In Figure 26 the performance of the ESH laminate at two different fiber contents can be seen. The fiber volume content had little effect on the laminate with ply drops, contrary to the significant effect reported for control materials [50]. The low fiber content control DD5 laminate with no ply drop has an S-N curve slope of about 10% of the static strength per decade of cycles. This fatigue performance is optimal for glass fiber composites, and is used as a standard to compare other laminates [50]. The delamination rates and lifetimes for the laminates containing ply drops are about the same for both low and high fiber contents. This is contrary to fiberglass laminates without ply-drops previously tested (DD5 & DD7), Mandell, et.al. [50], which

